Radiocarbon ages of dissolved and particulate organic matter in small water bodies of the Lena Delta

Number of Pages 41

Number of Fig. 20, Number of Tab. 11, Number of Appendix 5

provided as

Bachelorthesis

at

Institut für Geowissenschaften

der Rheinischen Friedrich-Wilhelms-Universität Bonn

by

Jens Steffen Hammes

Supervisors: Prof. Dr. Barbara Reichert

Prof. Dr. Gesine Mollenhauer

Bonn, [09/2019]

Hiermit erkläre ich, dass ich die vorliegende Arbeit selbstständig verfasst und keine anderen als die angegebenen Quellen und Hilfsmittel verwendet habe.

Bonn, den 26.9.2019

_____

Jens Steffen Hammes

Abstract

The term "Permafrost" describes soil or rock, whose temperature stays at or underneath 0 for at least two years. 50% of the globally estimated, soil-stored organic carbon is to be found in permafrost of the northern hemisphere

 Due to global warming more and more of this permanently frozen soil thaws. This leads to thermokarst processes, which create lakes and small ponds. Those lakes and ponds lead to more thawing of the soil around them. The long stored old organic material can be leached out by this thawing processes and either dissolve or float as particles in the water column.

Carbon, which is released in big arctic rivers, has been analyzed. Often, the particulate organic carbon (POC) carried by rivers is older than the dissolved organic Carbon (DOC). The radiogenic carbon signature of DOC shows a very young signature. Due to mineralization and metabolism by microorganisms large amount of DOC leave the flows as CO_2 and CH_4.

Concentrations of DOC in artic lakes have been analyzed while the origin of this DOC was completely unclear. Also, DOC from ponds has not been analyzed concerning their radiogenic carbon signature yet.

This bachelor thesis focuses on this gap of research and will attempt to answer the following questions: Do relations between the sizes of water bodies, the concentrations and radiogenic signature of DOC exist? What happens with dissolved and particulate carbon in lakes and ponds? Why carbon in artic rivers is so young?

The samples for this thesis were taken during field expeditions in August 2016 and July 2017. These expeditions took place in the central part of the Delta Lena. Samples were taken on the geological first terrace unit and on the third terrace unit. To cover the first terrace unit, lakes and ponds on Samoylov were sampled. To cover the third terrace unit, lakes and outflows on Kurungnakh were sampled.

To extract DOC the water samples were evaporated using a Rotary-Evaporator and afterwards analyzed in an AMS called MICADAS.

The resulting concentrations and radiogenic carbon signatures lead to the perception, that bigger lakes have a lower concentration of DOC with more enriched amounts of ^{14}C while smaller ponds have a higher concentration with a more depleted ratio.

DOC, which was leached into the waterbodies either gassed out due to mineralization or metabolisms by microorganisms. Bigger amounts of POC are especially leached into waterbodies due to heavy rain events, the thawing process in early summer and floods.

The enriched Δ^{14}C-signature of the Lena can be explained with the release of larger amounts of carbon with enriched Δ^{14}C-values from the first terrace. Additionally, older organic Carbon is instable and degrades fast.

Zusammenfassung

50% des geschätzten global im Boden gespeicherten organischen Kohlenstoffs befindet sich in Permafrostböden der nördlichen Hemisphäre. Böden die für mindestens zwei Jahre eine Temperatur um 0°C oder weniger aufweisen, werden Permafrostböden genannt. Diese Definition trifft auf 20 % der globalen Landmassen zu. Durch die globale Erwärmung beginnen mehr und mehr Permafrostgebiete zu tauen. Dies führt zu Thermokarstprozessen, durch welche Seen und Teiche entstehen. Durch die Bildung von Seen und kleineren Wasserkörpern taut umliegender Boden schneller auf.

Organisches Material, das in diesem Boden gespeichert ist, kann durch Tauprozesse gelöst oder auch partikulär in die Wassersäule der Seen und Flüsse gelangen. Über gelösten und partikulären Kohlenstoff in den größeren arktischen Flüssen ist bereits schon einiges bekannt. Zusätzlich wurde durch einige wissenschaftliche Veröffentlichungen eine moderne Signatur des, in den Flüssen gelösten, organischen Kohlenstoffs gefunden. Durch die Umsetzung dieses gelösten, organischen Kohlenstoffs können große Mengen an Kohlenstoffdioxid und Methan an die Atmosphäre abgegeben werden.

Konzentrationen von DOC in arktischen Seen wurde bereits analysiert, jedoch ist deren Ursprung noch relativ unklar. Ebenso ist die radiogene Kohlenstoff-Signatur von DOC in Teichen und Tümpeln unbekannt.

Diese Bachelorarbeit befasst sich mit dieser Forschungslücke und versucht auf die folgenden Fragen Antworten zu finden:

Bestehen Zusammenhänge zwischen der Größe eines Wasserkörpers, der Konzentration und der radiogenen DOC Signatur? Was passiert mit DOC und POC in Seen und Tümpeln? Und schließlich auch: Warum ist Kohlenstoff in arktischen Flüssen so jung?

Die Proben für diese Arbeit wurden im Zuge von zwei Expeditionen im August 2016 und Juli 2017 im Zentrum des Lena Deltas genommen. Beprobt wurden zwei verschiedene geologische Einheiten. Auf der einen Seite die erste Terrasseneinheit auf Samoylov. Auf der anderen Seite die dritte Terrassen Einheit auf Kurungnakh.

Im Labor wurde DOC aus den entnommenen Wasserproben mit Hilfe eines Rotationsverdampfers extrahiert und mithilfe eines Beschleuniger-Massenspektrometers bestimmt.

Die resultierenden DOC-Konzentrationen und ^{14}C-Signaturen führen zur Annahme, dass größere Wasserkörper wie Seen eine niedrigere DOC-Konzentration und eine leicht verarmte Menge an ^{14}C enthalten, wohingegen kleinere Wasserkörper wie Teiche und Tümpel eine hohe DOC-Konzentration und angereicherte Vorkommen an ^{14}C vorweisen.

DOC, das aus den Böden ausgewaschen wurde, gast entweder durch Mineralisierung aus oder wird von Mikroorganismen umgesetzt und als CO_2 oder CH_4 in die Atmosphäre freigesetzt. Größere Mengen an POC werden vor allem durch starke Regenfälle, durch das im Frühjahr stattfinden Auftauen und den damit verbundenen Überflutungen aus den Böden ausgewaschen und in Wasserkörper, Abflüsse und den Fluss Lena eingetragen.

Die moderne ^{14}C-Signatur der arktischen Flüsse kann durch die anteilig größere Menge von mit dem Radioisotop ^{14}C angereichertem Kohlenstoff von Inseln der ersten Terrasse erklärt werden. Die angereicherten Kohlenstoffverbingungen, die durch Abflüssen von Inseln der dritten Terrasse stammen, sind sehr instabil und zerfallen sehr schnell zu CO_2 und Methan.

Table of Contents

List of Figures

List of Tables

List of Appendix

Index of shortcuts

Index for shortcuts, units and symbols

<u>Units</u>

mbar	millibar
ml	milliliters
µl	microliter
m	meter
mm	millimeter
µm	micrometer
km	kilometer
km^2	square kilometer
kg	kilogram
g	gram
µg	microgram
Pg	petagram
Gt	gigaton
u	atomic weight
°C	Celsius

<u>Symbols</u>

‰	per mil
%	per centage
$\lambda^{14}C$	Half-life of Carbon isotope 14

Verzeichnis der verwendeten Programme

Grapher 10

Microsoft Excel

Microsoft PowerPoint

Microsoft Word

Quantum GIS Madeira 3.4

Acknowledgments

1   Introduction

Ground (soil or rock) whose temperature stays at or below 0 °C for at least two years can be considered as permafrost (Harris 1988). This definition applies to 20 % of the world's landmasses (French 2007). The estimated amount of organic carbon deposited in northern permafrost is 1700 Pg, which equals 50 % of the estimated global organic carbon being stored in the ground (Tarnocai et al. 2009). Around 400 Gt of this organic carbon is stored solely in the Yedoma Ice Complex (Tarnocai et al. 2009). The greatest rates of warming and thawing have been detected in the coldest permafrost sites (e.g. Romanovsky et al. 2010). In the period from 1901 to 2010 the surface air temperature of the northern Hemisphere increased by 1.12 °C (Jones et al. 2012). Climate warming is a serious problem in most northern high-latitude permafrost regions (ACIA 2004). Due to degradation and melting of permafrost, a destabilization of ground and the local infrastructure arises. The coastal and lacustrine ridges erode and the stored carbon is released into water bodies in arctic areas. The input of organic carbon in to lakes ushers in a mineralization and emission of 30-80 % of the total organic carbon as CO_2 and Methane (Algesten et al. 2003; Frey 2005).

The ice-rich permafrost deposits are becoming increasingly vulnerable to degradation in a warming climate (Morgenstern 2013; Straus 2017). This degradation has existed for a few decades (Romanowsky 2010). Due to degradation and melting, the Polar Regions become wetter and the surface area of lakes and ponds increases (compare with Pokrovsky et al. 2011). Those waterbodies process large amounts of carbon from terrestrial sources, which results in emissions of CO_2 caused by a supersaturation of carbon and mycobacterial metabolism (McCallister 2012). Furthermore, this input also leads to an increase of carbon transport to rivers and the ocean (Spitzy and Leenheer 1991). Due to these events the northern permafrost regions might change from a carbon sink to a carbon source (Schuur et al. 2008). If old organic carbon, which has been stored for hundreds to thousands of years, is released, it could have a massive positive feedback on the global climate (Schuur et al. 2013; Vonk et al. 2013; Mann et al. 2015).

Most studies performed to thoroughly understand the release of carbon focused on large scale lakes (Duchemin et al. 1999; Jonsson et al. 2003; Åberg et al. 2004; McGuire et al. 2009). Only a few look at smaller lakes and ponds, which have also a big influence on the global carbon cycle (Boike et al. 2008; Abnizova et al. 2012). Most global atmospheric models do not include small ponds, because ponds are often too small for satellite measurements to detect (Abnizova et al. 2012). Additionally, it is still unknown if the dissolved organic carbon (DOC) in waterbodies like lakes and ponds is modern or from an ancient source.

Therefore, knowledge of the age and the exact origin of DOC is an important issue for understanding the permafrost degradation.

This study will focus on the age of DOC of lakes and polygons from the Lena Delta by answering the following questions:

Does a relationship exist between the size of a waterbody, the concentration of old organic carbon and the $\Delta\ ^{14}$C-signature?

What happens to old organic carbon which is leached from frozen soils?

- ➔ Does old organic carbon reach the Lena River?
- ➔ Is the old organic carbon re-mineralized before it reaches the Lena River?
- ➔ Why is DOC in arctic rivers so young if the rivers are flowing through soils, which store thousand year old carbon?

2   Study Area

2.1   Geographic Overview

The study area is located in northeast Siberia (Figure 1). The Lena Delta is the largest delta in the Arctic, with a size of 32,000 km^2 (Are and Reimnitz 2000). The river itself is the second largest river in the Arctic, with a length of 4,400 km (Holmes et al. 2011; Frey and McClelland 2009). The delta is underlain by and belongs to the continuous permafrost zone, with a thickness between 400-600 m (Romanovskii and Hubberten 2001). The average annual temperature of this permafrost is about -10 °C at a depth of 10 m. Observations of deeper permafrost show that the mean temperature increased by 0.3 to 1.3 °C from 2006 to 2011 (Boike et al. 2013, 2015).
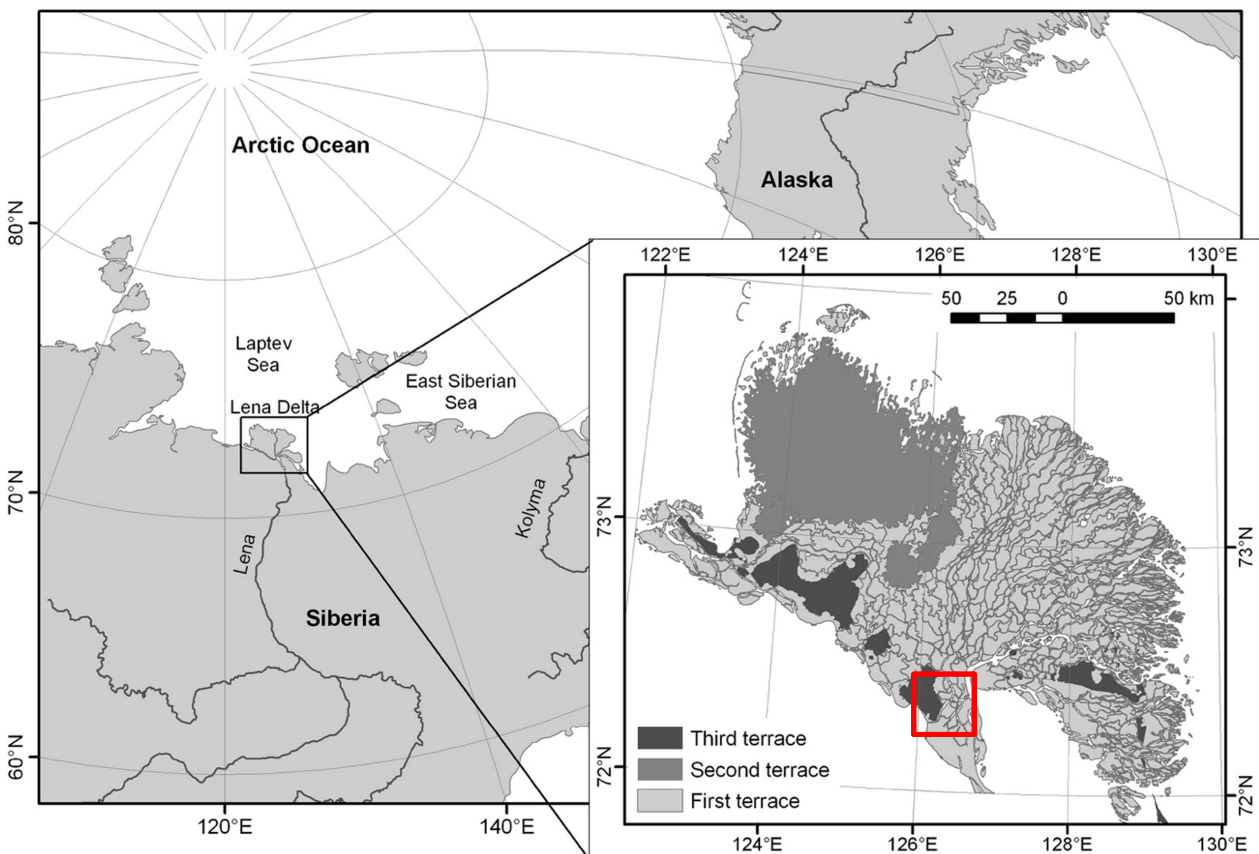
Figure 1:   Map of Siberia changed after Schneider et al. (2009)

The samples investigated in this study were taken from the islands of Samoylov and Kurungnakh, which are located in the southern central part of the delta. Samoylov is part of to the first terrace (Figure 2 upper right) and Kurungnakh consists mainly of deposits from the third terrace (Figure 2 lower left). Only a small part in the southwest of the island was deposited during the Holocene and therefore belongs to the first terrace.
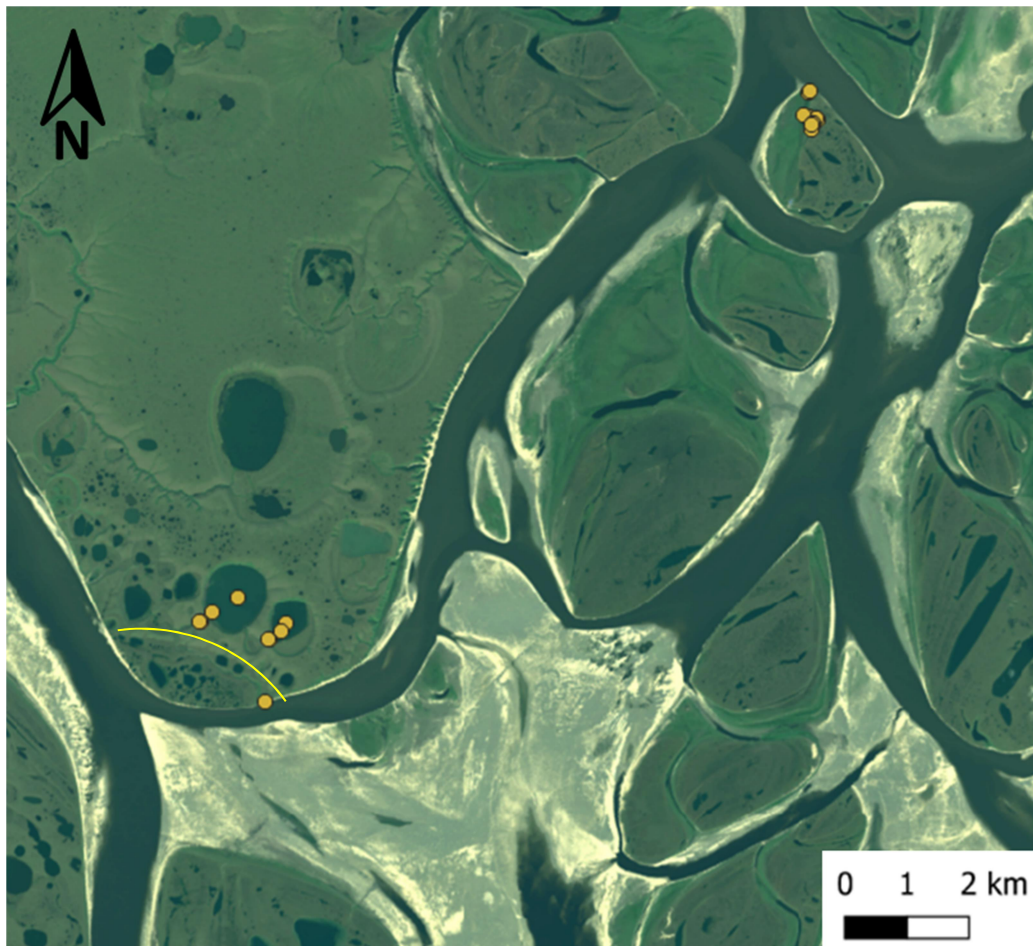
Figure 2: **Overview of the study sites and sampling locations. The island Samoylov is located in the upper right corner of this satellite picture and consists of Holocene first terrace deposits. The island Kurungnakh consisting mainly of third terrace units can be seen in the lower left. The yellow line broadly marks the border between the small first terrace southwestern part and third terrace (rest of the island) sediments of Kurungnakh (Changed after Sentinel-2 Picture from 06.08.2018)**

2.2   Climate

The climate of this region is classified as continental and Arctic since long winters (mean temperature in February 2011: -33.1 °C) alternate with short summers (mean temperature in July 2011: 10.1 °C) (Boike et al. 2013). The annual mean average temperature, measured at Samoylov Island, in the time period from 1998 to 2011 was -12.5 °C (Boike et al. 2013). The biggest temperature range was measured in the period of 2002 to 2011 with a low of -50 °C and a high of 20 °C (Langer 2013). The total amount of precipitation ranges from 72 mm per year measured in 1999 to 208 mm in 2003 (Boike et al. 2008). 45 % of this rain falls during the summertime (Wille et al. 2008).

2.3   Vegetation

The Lena Delta is in the tundra. The tundra is a transitional biome between the Taiga in lower Latitudes and the Arctic zone in higher Latitudes towards to the pole. Low temperatures and short growing seasons during unfrozen periods from June or July to September make it nearly impossible for trees and other bigger plants to grow (Harris et al. 1988). In these high Latitudes the vegetation (Figure 3) is limited to Lichens, Shrubs, Mosses, Grass, Rushes and Sedges (Elmendorf et al. 2012).

Figure 3: A picture that shows the typical vegetation of the tundra on Samoylov (picture taken by Anne Morgenstern).

2.4   Geology

The geology of the delta can be sub-classified into three different terraces (Schwamborn et al. 2002), each of which is portrayed by a different shade of grey in Figure 1. While the black color marks the third terrace, dark grey represents the locations of the second terrace and light grey those of the first terrace. The first terrace (1 to 12 m above the sea level) ranges over the main river and builds the eastern parts of the delta. It consists of fluvial sediments from mid-Holocene up to modern sedimentation and overlays a slide of debris. Its shape is characterized by ice-wedge polygonal tundra, active flood plains and thermokarst lakes (Fiedler et al. 2004; Schwamborn et al. 2002). Both ice-wedge polygonal tundra and thermokarst lakes are special structures, which occur in this area due to certain processes. The Ice-wedge polygonal tundra results from detritus transport and alluvial runoff from mountain valleys, valley slopes and cryoplanation terraces on hills (Schirrmeister et al. 2011). A mixture of fine-grained detritus, snow and plants is transported by meltwater and forms, after freeze and thaw cylces, an organic rich ice-complex (Schirrmeister et al. 2011). The cycles of thawing and freezing cause more transport by slope wash, solifluction and permafrost creeps. Alluvial and fluvial transport delivers increasing amounts of fine grain sediments and plant detritus (Schirrmeister et al. 2011). This leads to different ice deposits and the development of polygonal ice-wedges (Schirrmeister et al. 2011).

Thermokarst is defined as the process of thawing ground ice or ice-rich ground. Lakes and basins result out of this process and form a characteristic landscape (van Everdingen 2005). The soil collapses due to this thawing and leads to subsidence in the ground's surface. Water, which results from this thawing and meteoric rainfall, is collected in those basins and leads to more thawing. With more water the basin becomes a lake or pond. The soil as part of the ice complex underneath the new developed waterbodies with a few meter depth starts to thaw and builds up a so-called talik with a several tens of meters depth (West and Plug 2008) (Figure 4).

The second terrace consists of Late Pleistocene fluvial sediments and covers the northwestern part of the delta (Figure 1) at a height of 20-30 meters above sea level. The third and oldest terrace (30-55 meters above the sea level) is exposed in the south-southwestern part of the delta (Figure 1). This terrace is built by erosional remnants of an accumulation plain from the Middle to Late Pleistocene.

The third terrace on Kurungnakh can be divided into different units. The oldest includes fluvial sand, which was deposited in the early Weichselian (100.000 -50.000 BP). The next unit appears above as the Yedoma ice complex. It was formed during the middle and late Weichselian (44.500-17.000 BP) and consists of frozen peaty silt layers with large peat lenses. The youngest unit derives from the Holocene and consists of silty-sandy peat and deposits of thermokarst (Wetterich 2008).
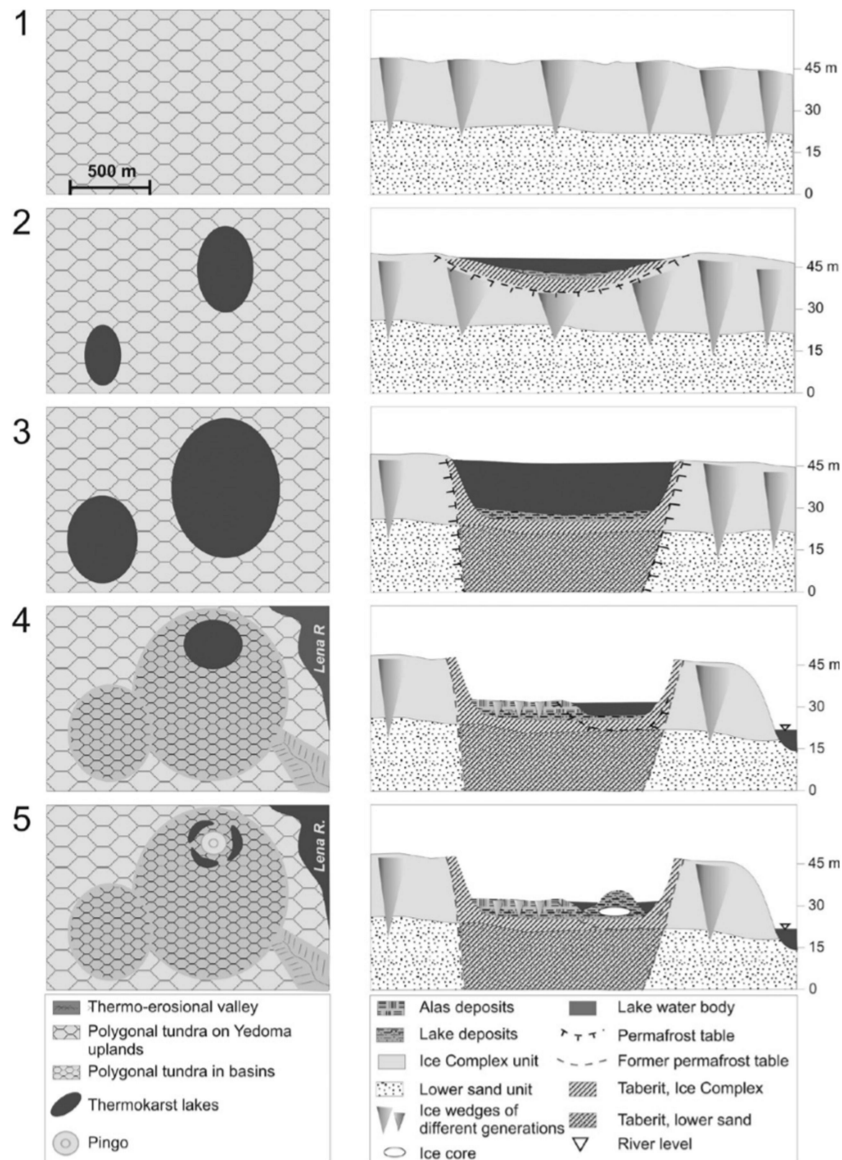
Figure 4: **Different development stages of a thermokarst lake in the Yedoma landscape (Morgenstern et al. 2011): 1: polygonal tundra. 2: melting leads to a development with lateral and vertical expansion and sedimentation. The talik starts to develop. 3: The mature stage of a thermokarst lake with only lateral expansion and lacustrine sedimentation. The talik is completely developed. 4: The lake starts to drain until a smaller lake remains or a new generation develops in the basin. 5: The thermokarst lake is drained and only some relict lakes and a pingo remain.**

2.5 Hydrogeography

The lakes formed by thermokarst in the Lena Delta are usually not deeper than 5 m (Boike et al. 2015). The diameter size of those lakes ranges from a few 100 meters to several kilometers (Grosse et al. 2013). Polygons are more dominant on islands of the first terrace then on islands of the third (Dr. Anne Morgenstern, Alfred Wegener Institute, pers. Comm. 2019). The ponds I focused on are not connected by surface channels. However, the lakes on Samoylov and on Kurungnakh are connected to each other and lead to an outflow at the coastline to the Lena River.

2.6 Study sites/study area

2.6.1 Samoylov

Samoylov belongs to the first terrace and can be divided in two different parts (Figure 5). The western greenish part of the island is the floodplain. This part is dominated by flood events which mainly occur during the thawing period at the beginning of summer but also due to heavy rain events, which only can happen in summertime (Wille et al. 2008). The eastern part belongs to older first terrace sediments and is embossed by the polygonal tundra landscape with thermokarst lakes and ponds.
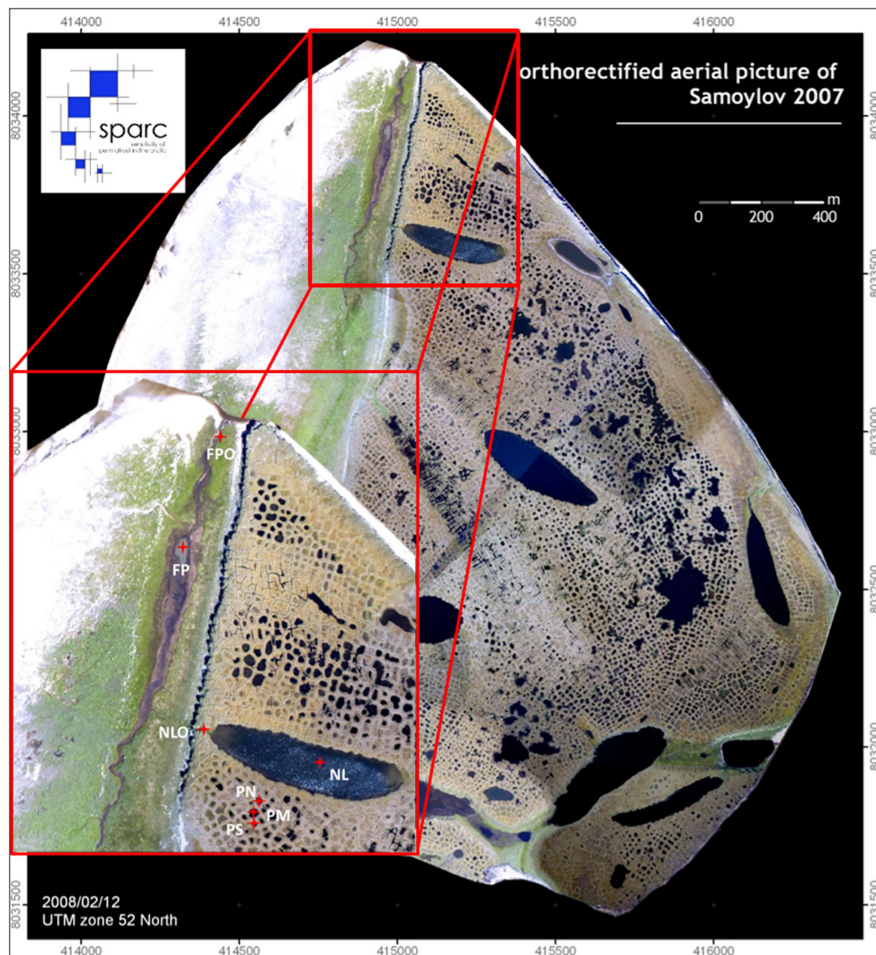
Figure 5: Orthomosaic picture of Samoylov from 2007 (modified after Boike 2012). The enhanced cutaway shows a precise overview of the sampled locations ("PS" Polygon South; "PM" Polygone Middle; "PN" Polygone North; "NL" North Lake; "NLO" North Lake Outflow; "FP" Floodplain; "FPO" Floodplain Outflow)

Polygon south, in the following shortened to "PS", Polygon Middle shortened to "PM" and Polygon North shortened to PN (Figure 5) represent typical ponds of the polygonal tundra in the southern part of

the zoomed in portion of the figure. The diameter accounts only a few meters. A bigger thermokarst lake on Samoylov is called North Lake and is abbreviated as "NL". Its outflow, shortened to "NLO", is a good example for the connection between the eastern higher plain and the western floodplain. As the water crosses the floodplain, it passes through a small lake called Katya Lake. After crossing the flood-plain, waters flow into the Lena River branch near Samoylov at the outflow which is referred to as "FPO" (floodplain outflow).

2.6.2 Kurungnakh

Figure 6 depicts the southern part of Kurungnakh. The two larger lakes denoted in figure 6 are thermo-karstlakes. The first lake in flow direction is called Oval Lake (surface area: 450,134.6 m^2 (Polakowski 2015)), shortened in figure 6 to "OV". This lake is partly drained (like in Figure 4 stage 4 shown) and its outflow is an inflow to the bigger lake to the west called Lucky Lake (LL) (surface area: 1,228,688.9 m^2 (Polakowski 2015)). The soil around the Lucky Lake degrades and erodes, introducing third terrace sedi-ments into the lake. Two further inflows to the Lucky Lake can be seen to the northeast. From Lucky Lake the water flows down on the first terrace (border to the first terrace: yellow mark in figure 6). This stream has inflows from the third and fist terrace. Two smaller lakes on the first terrace are also con-nected to the down flowing stream. Shortly before the stream reaches the outlet at the south coast of Kurungnakh, another lake from the third terrace adds water to the stream.
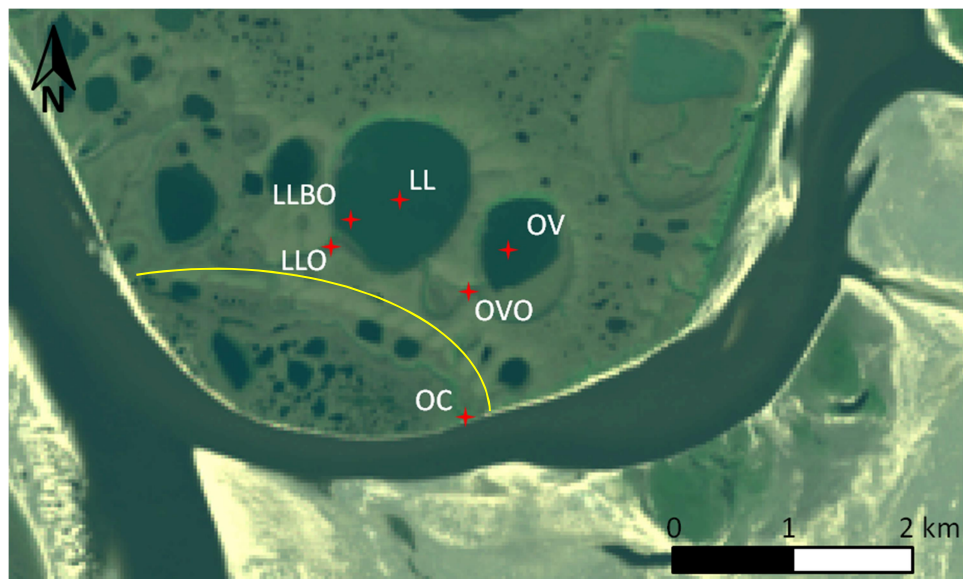
Figure 6: Satellite picture of Kurungnakh with locations of sampling. The yellow line broadly marks the border between the first terrace (small southwestern part) and third terrace (rest of the island) sediments of Kurungnakh (Changed after Sentinel-2 Picture from 06.08.2018)

3 Scientific background

Studies about the arctic regions and the permafrost in norther hemisphere are getting more and more important. One of the first expeditions of German scientists in cooperation with scientists from Russia to Sibiria took place in 1993. Since this first expedition more and more researcher teams explored different aspects of this region. Since at least the global warming became more and more significant, researchers started to focus more on studies of the Siberian permafrost. The extreme amounts of stored carbon in the soils and ice of the permafrost region gave scientists the question what would happen if those thaw. What could happen and how will it change the region and the rest of the world.

The geology and the way the Lena Delta and the local Ice Complexes formed were studied by Schwarmborn (2002), Schirrmeister (2011a; 2011b) and others. Mentioning Ice Complexes and the Lena Delta a few more specific informations about the hydrogeology, the polygonal tundra and thermokarst lakes were published by Julia Boike (2012; 2013; 2015; 2019) and Anne Morgenstern(2011; 2013).

Based on a 36-year observation period Kirpton et al. (2011) demonstrated that the total lake areas in West-Siberia increased and that the land became wetter. The wetter the area becomes, the more the surface area of lakes and ponds increases (Pokrovsky et al. 2011). The more the surface area of lakes and ponds increases the more carbon can be mobilized and emitted. Even if they are not connected by surface outlets, they release carbon. The amount of carbon leaving the system by outgassing of waterbodies is higher than the amount which could leave it through lateral run offs (Abnizova et al. 2012).

In Studies which focus on the utilization of leached out carbon, arctic rivers are compared to conduits which bring carbon to the coastal areas and artic oceans (Mann et al. 2015). This ancient carbon (>20,000 B.P.) is rapidly utilized by microbes (Spencer et al. 2015). Spencer et al (2015) showed that 50 % of the ancient carbon was utilized within 7 days with a decay rate of 0.12 to 0.19 % per day in arctic rivers. Other studies, such as Åberg et al. (2004) or McGuire et al. (2009) focus also mainly on arctic rivers or bigger lakes. Research on terrestrial smaller waterbodies with an increasing appearance is not equally covered. Especially the age of carbon, which is released and dissolved in waterbodies with a small surface area, is not investigated.

First DOC concentrations were measured and sampled by Polakowski (2015) on Kurungnakh.

4   Methods

4.1   Sampling

The samples for my project were taken during the 2016 Lena expedition, by Thorsten Riedel and Vera Meyer (Riedel 2016) and during the 2017 Lena expedition by Maria Winterfeld and Hendrik Grotheer (Winterfeld et al. 2017). The expedition in 2016 started on 1st of August and ended on 31st of August. The 2017 expedition started on the 2nd of July and ended on the 31st of July. The teams collected various sample types. Samples were taken from the Lena River, on Samoylov from North Lake and some nearby polygons, and on Kurungnakh of Oval Lake, Lucky Lake and inlets and outflows of these Waterbodies (Figures 7 and 8). Samples of various depths were taken in the lakes and the Lena River.
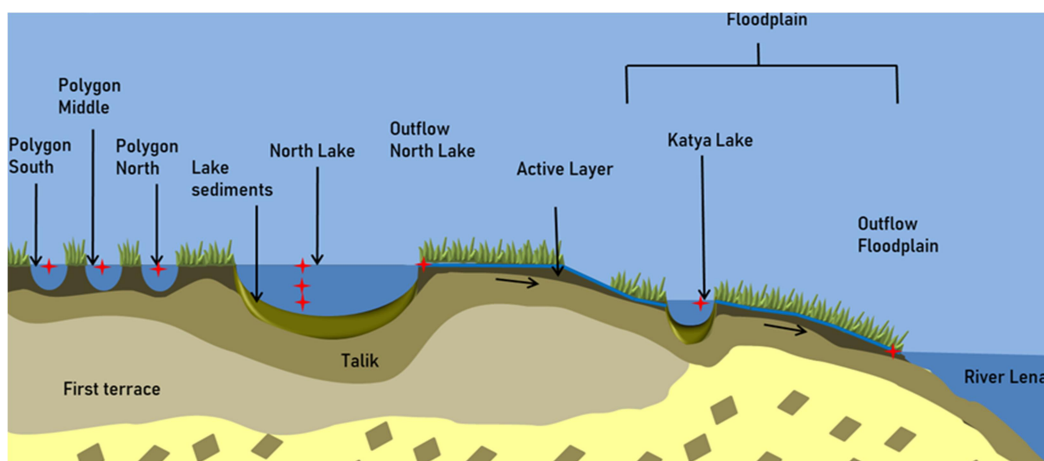
Figure 7:   Conceptual model of Samoylov. Polygons sampled for this study are displayed from south to north. Lakes, outflows and streams are portrayed in the order of the flow direction to Lena River.
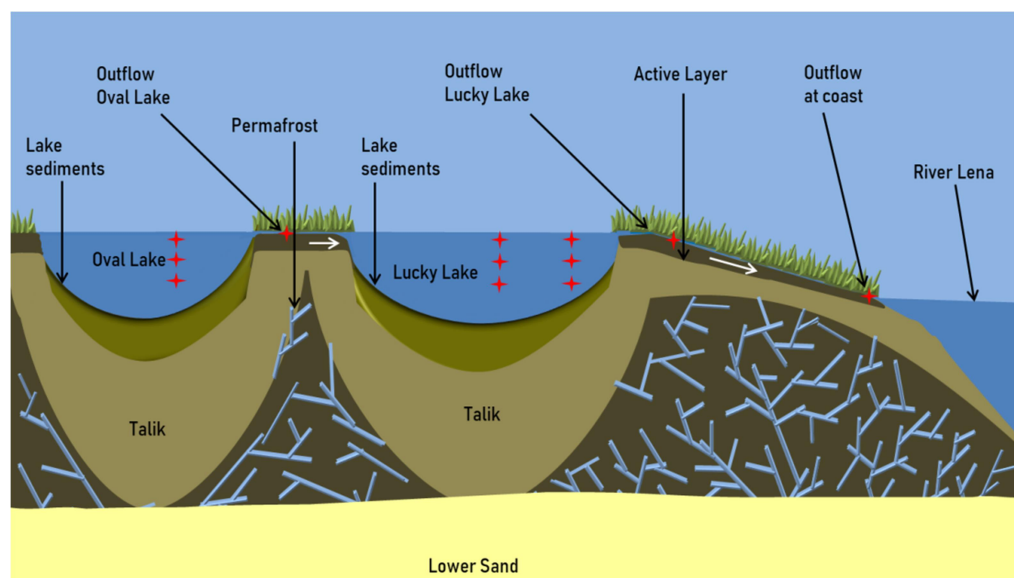
Figure 8:   Conceptual Model of Kurungnakh. Lakes, Outflows and streams are shown in in the order that arises out of the flow direction to Lena River.

A standard Niskin water sampler (General Oceanics model 1010) with 5-liter capacity was used for sampling. The close mechanism of the sampler was triggered by a 400 g drop messenger. The sampler was weighted down by a 15 kg iron weight and lowered with a 30 m long rope. To avoid the mixing of stratified waterbodies the engine of the boat was switched off during sampling and the extraction of water started first at the surface and then to consecutively deeper positions. The collected water was trans-

ported in 10 to 20 l jerrycans in 2016 and in 15 to 20 l plastic canisters in 2017. These vessels were cleaned by rinsing with tap water in the lab and water at the sampling locations, respectively.

Several kinds of filters were used. Some samples were filtered through a 0.7 µm glass fiber filter (GFF) and others through a 0.45 µm GFF. Those filters had been combusted before the trip at 450 °C for 4.5 hours. The filters with 0.7 µm pore size have only been analyzed for one location, because no other filters exist for this site. 0.45 µm filters of 2 different diameters were used in the field. The smaller filter has a diameter of 25mm. The larger filter with a pore size of 0.45 µm has a diameter of 47mm. The 47 mm diameter filters were used on a filter apparatus designed for 25 mm filters after the larger filter apparatus accidentally broke. Tables 1 and 2 provide an overview of samples taken.

Before the filtration in the field laboratory started, the rack and flask were rinsed with 30 ml of MilliQ water. For each sample, 3 times 60 ml was filtered through 47 mm and 25 mm filters in 2016. In 2017, for some samples 400 ml was filtered and for others 200 ml. The filtrated water samples were frozen after filling them into HDPE bottles. Further information about the expeditions can be found in the expedition reports by Riedel (2016) and Winterfeld et al. (2017).

Table 1:   List of samples from Samoylov analyzed in this study

Sample Origin	Sampling Date	Depth	Type of sample	Volume [ml]	Coordinates
Polygon South	10.08.2016	0 m	1x 0.45 µm DOC 1x 0.45 µm POC Filter (1/2 47 mm)	60	N 72,3836 E 126,4856
	14.07.2017	0 m	1x 0.45 µm DOC 1x 0.45 µm POC Filter	200	
Polygon Middle	10.08.2016	0 m	1x 0.45 µm DOC 1x 0.45 µm POC Filter (1/2 47 mm)	90	N 72,3837 E 126,4855
	14.07.2017	0 m	1x 0.45 µm DOC 1x 0.45 µm POC Filter	200	
Polygon North	10.08.2016	0 m	1x 0.45 µm DOC 1x 0.45 µm POC Filter (1/2 47 mm)	90	N 72,3839 E 126,4858
	14.07.2017	0 m	1x 0.45 µm DOC 1x 0.45 µm POC Filter	200	
North Lake center	10.08.2016	0 m; 3.7 m	2x 0.45 µm DOC 2x 0.45 µm POC Filter (1/2 47 mm)	90	N 72,3845 E 126,4890
	08.07.2017	0 m; 1.5 m; 3 m	3x 0.45 µm DOC 3x 0.45 µm POC Filter	400	
North Lake outflow	10.08.2016	0 m	1x 0.45 µm DOC 1x 0.45 µm POC Filter (1/2 47 mm)	90	N 72,3849 E 126,4829
	07.07.2017	0 m	1x 0.7 µm DOC 1x 0.7 µm POC Filter (1/4 25 mm)	400	
Floodplain	08.07.2017	0 m	1x 0.45 µm DOC 1x 0.45 µm POC Filter (1/4 25 mm)	400	N 72,3852 E 126,4805
Floodplain Outflow	18.08.2016	0 m	1x 0.45 µm DOC 1x 0.45 µm POC Filter (1/1 25 mm cut from 47 mm)	90	N 72,3889 E 126,4829
	08.07.2017	0 m	1x 0.45 µm DOC 1x 0.45 µm POC Filter (1/4 25 mm)	400	

Table 2: **List of samples from Kurungnakh analyzed in this study**

Sample Origin	Sampling Date	Depth	Type of sample	Volume [ml]	Coordinates
Oval Lake center	11.08.2016	0 m; 2.5 m; 3 m	3x 0.45 μm DOC 3x 0.45 μm POC Filter (1/1 25 mm cut from 47 mm)	90	N 72,2949 E 126,2028
	21.07.2017	0 m; 2 m; 4 m	3x 0.45 μm DOC 3x 0.45 μm POC Filter (1/4 25 mm)	400	
Oval Lake Outflow	11.08.2016	0 m	1x 0.45 μm DOC 1x 0.45 μm POC Filter (1/1 25 mm cut from 47 mm)	90	N 72,2920 E 126,1942
	21.07.2017	0 m	1x 0.45 μm DOC 1x 0.45 μm POC Filter (1/4 25mm)	400	
Lucky Lake center	11.08.2016	0 m; 2 m;3,5-3,7 m	3x 0.45 μm DOC 3x 0.45 μm POC Filter (1/1 25 mm cut from 47 mm)	90	N 72,2987 E 126,1751
	24.07.2017	0 m; 1.5 m; 3 m	3x 0.45 μm DOC 3x 0.45 μm POC Filter (1/4 25 mm)	400	
Lucky Lake before Outflow	11.08.2016	0 m; 2 m; 3,3 m	3x 0.45 μm DOC 3x 0.45 μm POC Filter (1/1 25 mm cut from 47 mm)	90	N 72,2962 E 126,1611
Lucky Lake Outflow	11.08.2016	0 m	1x 0.45 μm DOC 1x 0.45 μm POC Filter (1/1 25 mm cut from 47 mm)	90	N 72,2944 E 126,1550
	21.07.2017	0 m	1x 0.45 μm DOC 1x 0.45 μm POC Filter (1/4 25 mm)	400	
Outflow at coast	21.07.2017	0 m	1x 0.45 μm DOC 2x 0.45 μm POC Filter (1/4 25 mm) (1/8 25 mm)	200	N 72,2814 E 126,193

4.2 Sample Preparation

The dissolved organic carbon concentration was analyzed by Claudia Burau (Section Ecological Chemistry, Alfred Wegener Institute, Bremerhaven) using a Shimadzu TOC-VCPN analyzer.

For radiocarbon (^{14}C) analyses, DOM needed to be extracted from the samples. This was done by drying the samples using rotary evaporation (Roto-evaporation). The sample volume required for ^{14}C analyses of DOC was calculated based on the concentrations according to formula (1)

$$(1)\ V_{sample} = \frac{100\ \mu gC}{c_{sample}*A_c} * 1000 \qquad\qquad (1)$$

V_{sample} Volume needed for extracting 100 µg of carbon in [ml]
c_{sample} Concentration of sample in [µM]
A_c Atom mass of carbon [12.0107 u]

Roto-evaporation (RV)

A sample volume corresponding to 100 µg C as DOC was transferred into a 25 mL pear-shaped flak using a glass pipette. For those samples, for which a volume >25 mL was required, a first aliquot of 20 mL was filled into the pear-shaped flask and dried. The remaining sample volume was then added to the dried extract. Samples were dried using a Heidolph LABORATA (roto-evaporation apparatus) (Figure 9). Prior to sample evaporation, the apparatus was cleaned by attaching a round-bottom flask filled with 200 ml of Milli-q water (EMSURE Water for analysis). After the 200 mL had evaporated, the connections and the surfaces, where the flask is attached to the vapor tube were cleaned with Isopropanol.
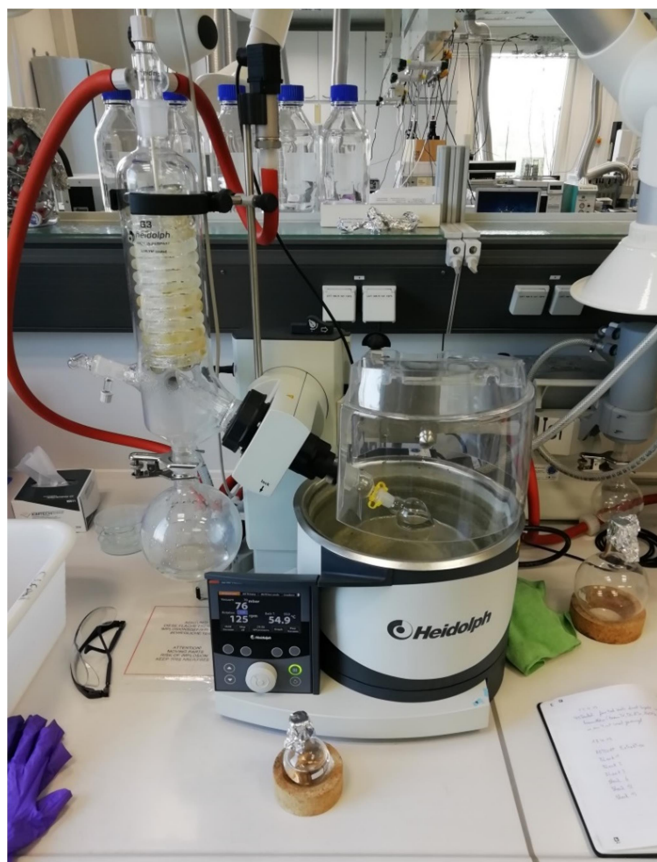
Figure 9: Rotary-Evaporator in Action

After the cleaning process, the pear-shaped flask was attached to the vapor tube, which was connected to condenser unit. The water bath was set to a temperature of 60 °C. The pressure setting for the vacuum was 70 mbar with a delta pressure of 20 mbar (compare to Grotheer 2012)). The pear-shaped flask

rotated 120 times per minute. Pear-shaped flasks that were filled with up to 20 ml needed 10 minutes to warm up. In order to slowly increase the temperature to avoid boiling retardation, the flask was lowered so that it just touched the surface of the warm water bath. After 10 minutes, the flask was lowered inside the water bath with no danger of boiling. The evaporation is finished when only a small amount of water remains in the flask (ca. 1 ml). Then, rotary-evaporation was stopped and the rest of the sample was transferred with Milli-q water from the flask into a 4 ml-vial. The LABORATA ran a cleaning run with 50 ml Milli-q water between each sample. After this washing run, the surfaces of the connecting parts were cleaned again with isopropanol.

The 4 ml-vials were dried on a heating plate underneath a flow of nitrogen until no visible remains of liquid could be observed. After this drying process, the residue was re-dissolved in Milli-q water (50 µl) and transferred into tin capsules. This transfer was repeated three times. The tin capsules were dried in a desiccator for minimum of 3 hours at 60 °C. After the last drying process the tin capsules were folded into cubes for combustion in the EA.

Preparation of glass fiber filters

The filters, which have been used in the field to filter the water sample, can be used to determine the concentration of particulate organic carbon (POC). The filters were cut to the following sizes after thawing and drying in a 40 °C oven for at least 12 hours. All 47 mm filters were cut in half, because that is the maximum size which fits into an 8x8x15 mm tin boat. Those 47 mm filters, which were used on a filtration device designed for 25 mm filters, which were only covered with particles in the center, were punched using a 25 mm circular hole punch. These punches as well as the 25 mm diameter filters were cut in quarters, because of a higher concentration on a smaller filter.

After cutting, the filters were acidified with drops of a one molar hydrochloric acid, with a glass pipet (Table 3). Filter acidification removes possible carbonate particles, which could contaminate the measurements of POC.

Number of acid drops added to the filter samples

Filter size	1/2 47 mm 0.45 GFF	1/1 25 mm cut from 47 mm 0.45 GFF	1/4 25 mm 0.45 GFF	Outflow Kurungnakh 1/8 25 mm 0.45 GFF	Outflow Kurungnakh 1/4 25 mm 0.45 GFF
Number of acid drops	10-11	5-6	3-4	3	7

The acidified filters were dried overnight in a 40 °C oven. The following day they were packed in tin boats and pressed into small disks (Figure 10). Those disks were then combusted and analyzed for organic carbon concentration in the (EA) (Figure 9).

Figure 10: Pressing device for packed filters

4.2.1   Radiocarbon analysis

After packing the samples into tin boats and tin cups, they were loaded into the EAs sampler (Figure 11: red circle on top of the EA). In the EA samples are combusted under a constant flow of helium at 950°C. In addition to helium, oxygen is introduced to assure complete combustion to CO_2, H_2O, N_2, Nitrogen oxides (NO_x), SO_2 and SO_3. CO can also result from incomplete combustion. To increase the CO_2 yield, the mixture of gases is oxidized by a copper oxide. While silver wool in the combustion tube removes SO_2 and SO_3, and copper wire pieces reduce the nitrogen oxides to N_2 and water (which is then removed in a Sicapent water trap). The resulting gas mixture consists of CO_2 and N_2. This gas mixture is transmitted to the Gas Interface System (GIS) (Ruff et al. 2010). The GIS allows for the measurement of samples with a small amount of carbon in the Mini Carbon Dating System (MICADAS). The ideal amount of Carbon to for the best measurement is 100µg. The gas mixture is introduced into a gas stream of helium. CO_2 is adsorbed selectively by a zeolite trap. After it is captured, the trap is heated up to 450°C to release the CO_2. This CO_2 is fed into the stream of helium with a proportion of 2-5% of CO_2 and 95-98% of helium. The new mixed gas is transferred continuously into the gas ion source of MICADAS (Figure 12: No 1).

The inflowing gas is ionized with positively charged cesium ions. This leads to a stream of negatively charged ions from the sample. This process eliminates the chance of contamination through ^{14}N, because ^{14}N cannot produce anions. The resulting negatively charged carbon ion beam is focused by an array of focusing lenses and streams to the impactor magnet, which bends the beam by 90 degrees. In this bending, the different molecules are separated by mass. The separated negatively charged molecules are accelerated to a high positive potential inside the tandem accelerator. After acceleration they pass through the electron stripper, which positively charges the remaining molecules and divides them into fragments and carbon ions. This beam of fragments and carbon ions is subsequently deflected by a second magnet, the high-energy magnet. The deflection of the beam leads to another separation of carbon ions with the masses of ^{12}C, ^{13}C and [14]C. The fragments are sorted out before, while the Carbon ions stream to the last part of the AMS. These remaining ions are detected by measuring the ^{12}C and ^{13}C beams amperage using Faraday cups. The amount of ^{14}C cannot be measured with a Faraday cup, be-

cause the amperage of a ^{14}C is too low for the device. To solve this problem a gas ionization chamber is used to measure the ^{14}C ions. More detailed information can be found in Synal et al. (2007).
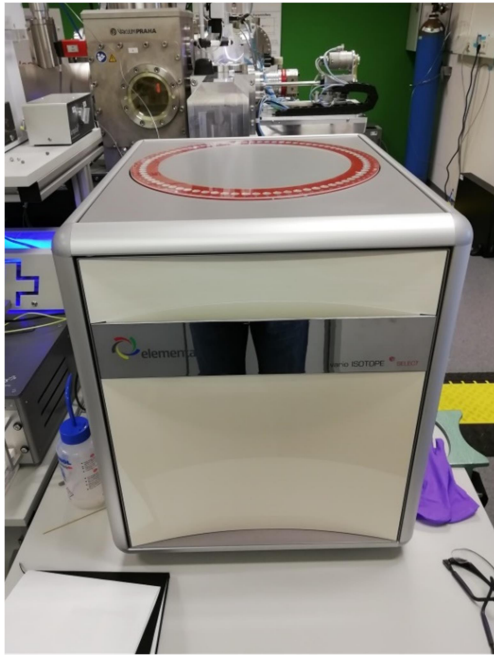
Figure 11: Picture of the Elementar Analyzer (EA)
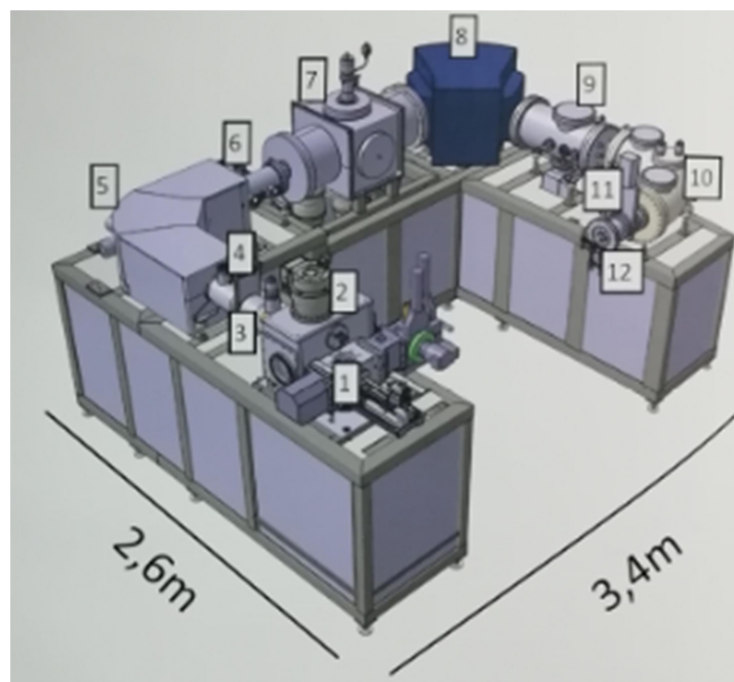
Figure 12: CRD sketch of MICADAS (awi.de)

5   Results

In the following chapter I will present my results separately for each of the two islands. The order of the sampling locations reflects the flow direction through the waterbodies towards the outflow at the coast of the island to the river Lena. On Samoylov the flow begins at the North Lake. In order to mention the data from the ponds as well, which are not connected to other waterbodies, I set them at the beginning in the order they are located on Samoylov from south to north. The different years are illustrated with different colors. Turquoise represents the year 2016 and red the year 2017. The different shapes are meant to emphasize the difference between DOC (rhomb) and POC (square) values. The X-axis of each diagram shows the location of sampling. The Y-axis changes between values for the concentration in mg/L of POC and DOC and signature of $\Delta ^{14}C$ for DOC and POC. The measured results of the MICADAS are listed in the Appendix 1. $\Delta ^{14}C$ values have been calculated with blank corrected $F^{14}C$ (Appendix 1).

5.1 Samoylov

DOC concentrations show a high variation between the samples ranging from 7.63 mg/L (Polygon South) in 2017 to 2.62 mg/L (North Lake 1.5m) in 2017 (Figure 13a). The DOC concentrations from the lake to the river in the year 2016 are slightly higher than those of 2017. The general trend of DOC concentration of Samoylov is higher in Polygons than in North Lake. From North Lake on, the DOC concentration increases towards the outflow at the coast.

The variation in the POC-concentration of the different samples is generally not smaller compared to DOC concentration despite one exception (Figure 13b). The exception comes from the Outflow of North Lake, with a POC concentration of 6.93 mg/L POC. The biggest difference between the POC concentrations without the sample of Outflow North Lakes is 1.82 mg/L between a sample from Polygon South 2016 (2.2 mg/L) and the Outflow at the Coast in 2017 (0.38 mg/L). The range of the other samples extends from 0.43 mg/L to 2.24 mg/L.

Samples from 2016 are higher in concentration at every location in comparison to those of 2017(Figure 13b). Additionally, the 2016 samples do not show a decrease in the concentration at the North Lake or other locations. The 2017 samples on the other hand show a nearly similar trend to the concentration of DOC samples on Samoylov, i.e., the concentration of the ponds are similar to each other (Polygon North 0.65 mg/L, Polygon Middle 0.62 mg/L and Polygon South 0.54 mg/L) and decrease in the direction of North Lake. Additionally, the concentration increases towards the floodplain (Figure 13b). The floodplain also has a similar concentration to the ponds. What differs from the trend of the DOC concentration is a decrease at the outflow of the floodplain. There the concentration is nearly the same as in North Lake.

The Δ^{14}C-signatures range from 60 to -10‰ (Figure 13c). The signatures of samples from 2017 are more depleted then those of samples of 2016. This relation is only opposite at Pound South. The three ponds have more modern signatures in both years than the rest of the sampled locations. The sample taken from Polygon North in 2017 differs from the other polygons, but has a nearly similar signature to the North Lake, the outflow of the lake, the floodplain and the outflow at the coast. Those samples differ from each other in their signature from 10 to -10‰, but less than the difference between them and the polygons with signatures of 46 to 60‰ (Figure 13c).

The Δ^{14}C signatures of POC of the samples from 2016 vary more strongly than those from 2017 (Figure 13 d). The minimum as well as the maximum of the Δ^{14}C signatures of POC are from the year 2016. The most depleted signatures of 2016 occur in North Lake and the youngest in its outflow. Compared to the Δ^{14}C-signatures of the atmosphere in 2016 and 2017 and the Δ^{14}C-signature of the oldest measured soil sample (Figure 13c and 13d), the signatures of 2017 range within a narrower range between -34‰ and -184‰. Notably, the signature of the deepest sample from North Lake has a more enriched Δ^{14}C-signature than the polygons. In contrast to that strong enriched signature the most depleted sample is located at the floodplain as marked in the graph of the DOC ^{14}C signatures.
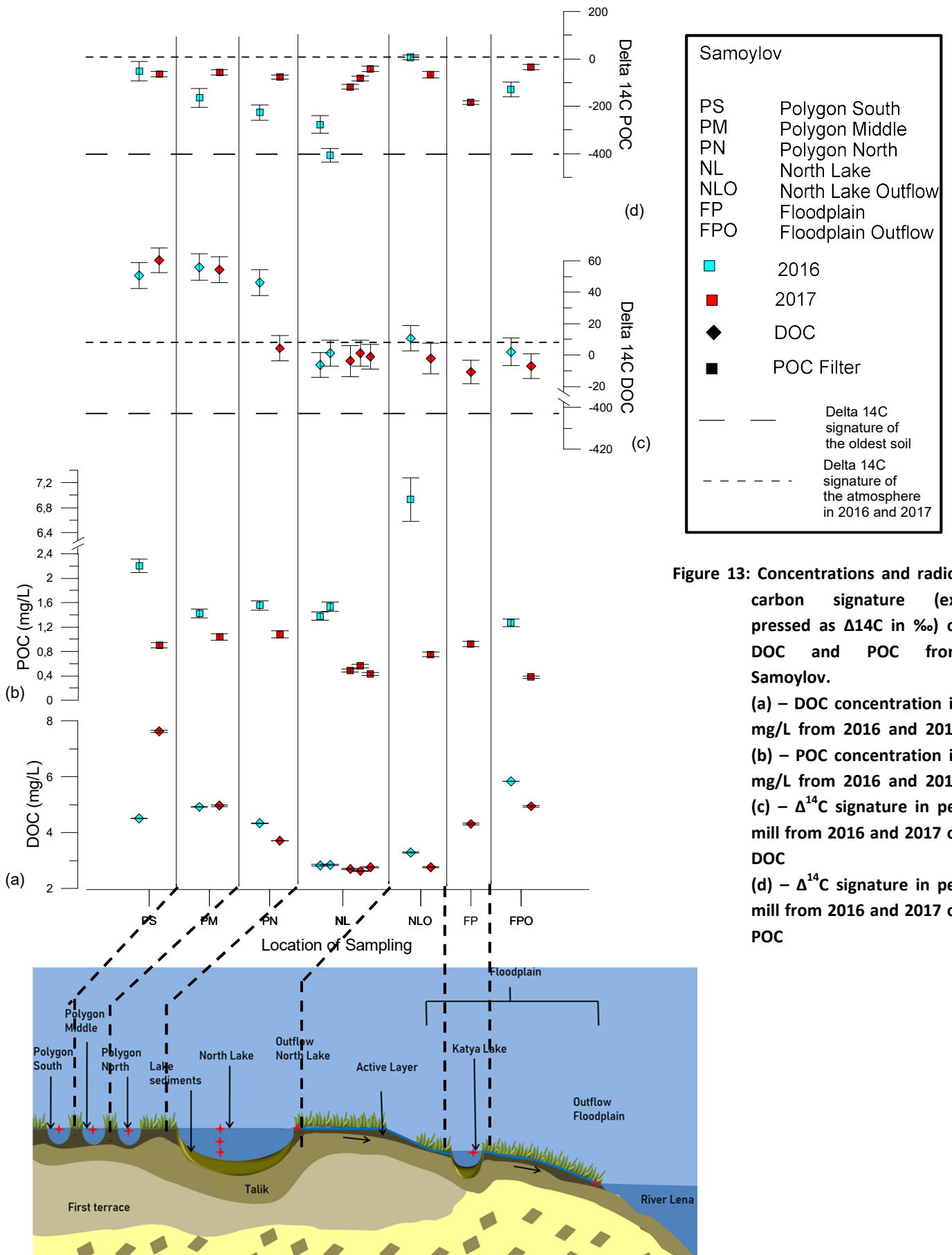
Figure 13: Concentrations and radio-carbon signature (expressed as Δ14C in ‰) of DOC and POC from Samoylov.
(a) – DOC concentration in mg/L from 2016 and 2017
(b) – POC concentration in mg/L from 2016 and 2017
(c) – Δ14C signature in per mill from 2016 and 2017 of DOC
(d) – Δ14C signature in per mill from 2016 and 2017 of POC

5.2 Kurungnakh

In Figure 14 the concentration and Δ^{14}C signature of DOC and POC from Kurungnakh is shown. The highest DOC concentration on Kurungnakh is 5.04 mg/L (Figure 14a). It was measured in a sample, taken from the center of Lucky Lake at a depth of 3m in 2016. In contrast, the sample with the lowest concentration was taken at the outflow to the Lena River in 2017(Figure 14a). Generally, the DOC concentrations of the sampling sites over both years are similar, except at Lucky Lake and Lucky Lake Outflow, where larger differences were observed. In 2016 the concentration of DOC in samples from Lucky Lake increased with depth. However in 2017 the samples' concentrations are nearly the same. The second bigger difference in concentration is at Lucky Lake Outflow. The sample from 2017 has a higher concentration than the one collected in 2016. The general trend of both years is the same. At the beginning of the flow on Kurungnakh the concentration is nearly the same in Oval Lake and its outflow. Afterwards the concentration increases in Lucky Lake and fro there decreases along the flow path to the outflow at the coast (Figure 14a).

The two measurements with the highest POC concentrations were taken from one filter in 2017 from the outflow to the Lena, which is covered by a dark organic rich layer (Figure 14b). The exact concentrations of those two measurements are 13.44 mg/L and 7.3 mg/L. The rest of the samples and measurements fit in a narrower range between 0.94 mg/L and 0.28 mg/L. The trend of Oval Lake and Outflow Oval Lake is similar to the trend observed in the concentration of DOC. At Lucky Lake the POC samples from 2016 are similar to those of Oval Lake and Outflow Oval Lake. In 2017 the concentration at Lucky Lake is higher at the surface (0.94 mg/L) and decreases with depth to 0.59 mg/L at 3m (Figure 14b). The concentration at the outflow of Lucky Lake reaches the lowest value on Kurungnakh.

The lowest Δ^{14}C per mil value was measured in a sample from Lucky Lake from 2016 with -384‰ (Figure 14c). The highest per mil value was measured in a water sample from Oval Lake Outflow in 2017 with -300‰. Generally, the graph looks like an inverse copy of the DOC concentration graph of Kurungnakh (Figure 14a). The samples from Oval Lake and Oval Lake Outflow have, together with the sample from the Outflow at the coast, the highest per Δ^{14}C values (Figure 14c). In contrast to this the Lucky Lake center has the most ^{14}C depleted signatures. In the continuing flow the signature becomes younger to the outflow at Lucky Lake and coast to the Lena River.

The range of different Δ^{14}C signatures for POC on Kurungnakh is immense with a difference of 302‰ (Figure 14d). The most enriched value (-126‰) was measured in 2016 in Lucky Lake at a depth of 3.5-3.7m (Figure 14d). The oldest signature was measured at the coastal outflow to Lena River with a Δ^{14}C signature of -428‰. The general trend of the Δ^{14}C signature of POC is decreasing towards the outflow to the Lena. From Oval Lake to Lucky Lake the signature becomes a little younger. Before the outflow it is older than at the outflow of Lucky Lake. The oldest signature was measured in samples of the outflow to the Lena River. While the DOC becomes younger towards the outflow in a small scale, the signature of POC is decreasing in a much larger scale (Figure 14d).
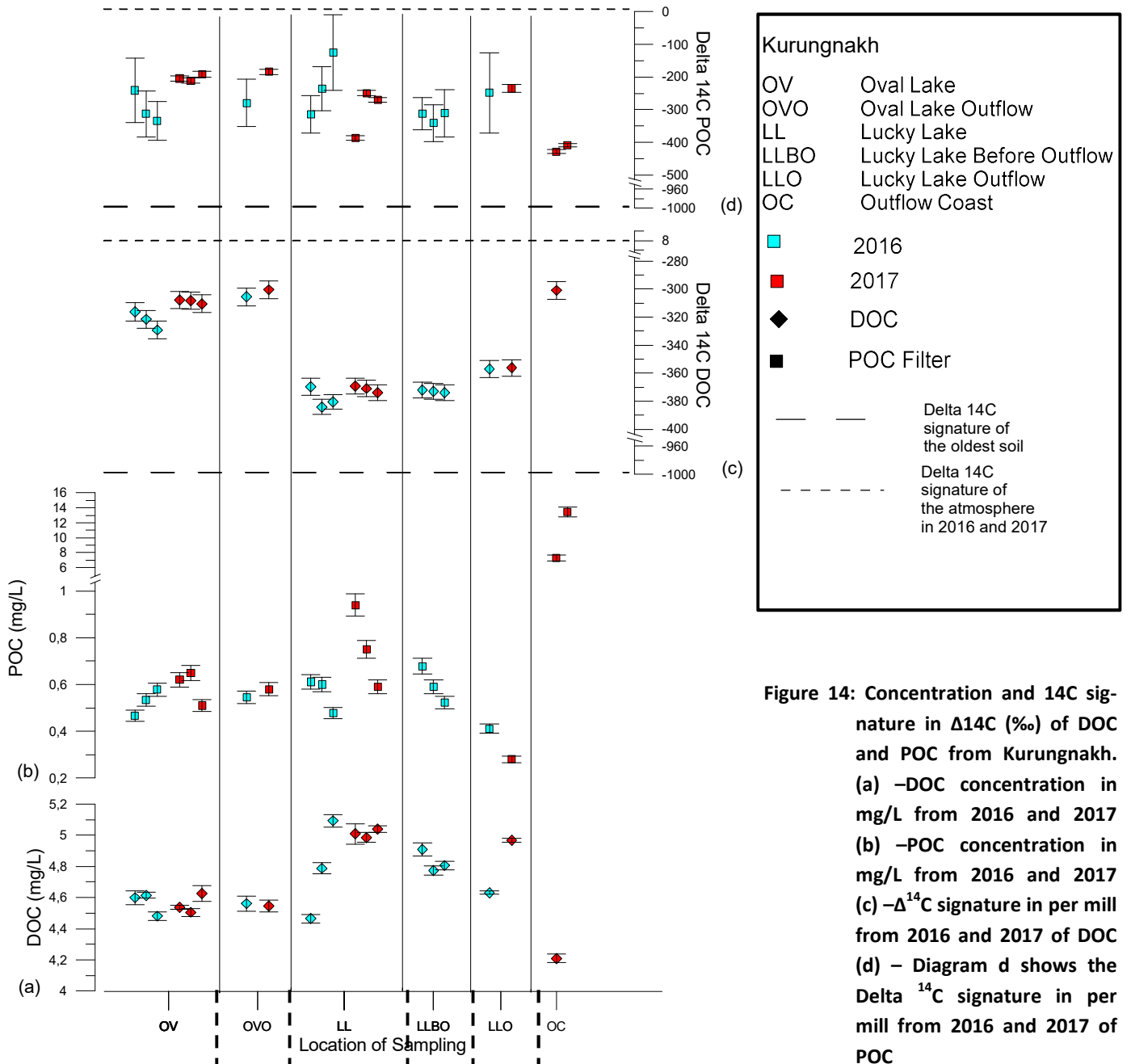
Figure 14: Concentration and 14C signature in Δ14C (‰) of DOC and POC from Kurungnakh. (a) –DOC concentration in mg/L from 2016 and 2017 (b) –POC concentration in mg/L from 2016 and 2017 (c) –Δ14C signature in per mill from 2016 and 2017 of DOC (d) – Diagram d shows the Delta 14C signature in per mill from 2016 and 2017 of POC
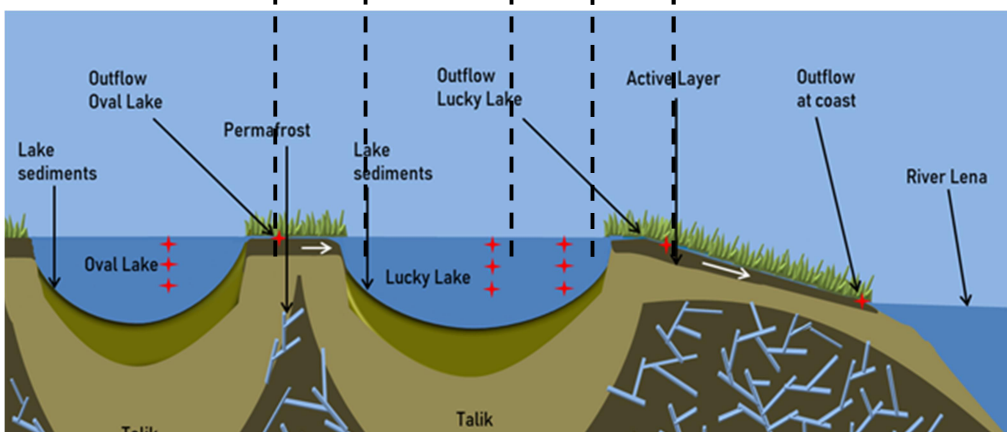
6   Discussion

The plotted and described values of DOC-, POC concentrations and their measured Δ^{14}C signatures show similarities and reoccurring differences. In this chapter those characteristics will be put into context by answering specific questions, which help to summarize the earned results.

Main factor at play between the samples exist between the terraces type and the sample locations (ponds vs lakes). The differences found due to the divergent hydrogeology and geology and may lead to certain connections between the sizes of waterbodies and DOC.

6.1   Does a relationship exist between the size of a water body, the DOC concentration and the Δ^{14}C signature on Samoylov?

Samoylov belongs to the First Terrace unit of the Lena Delta (Figure 15). On this island, concentrations and radiocarbon signatures of DOC in polygons and North Lake on Samoylov are distinctly different. The majority of the measurements from polygon samples show a high concentration of DOC (4.33 to 4.97 mg/L) whereas the lake has a lower concentration (2.62 to 3.29 mg/L).
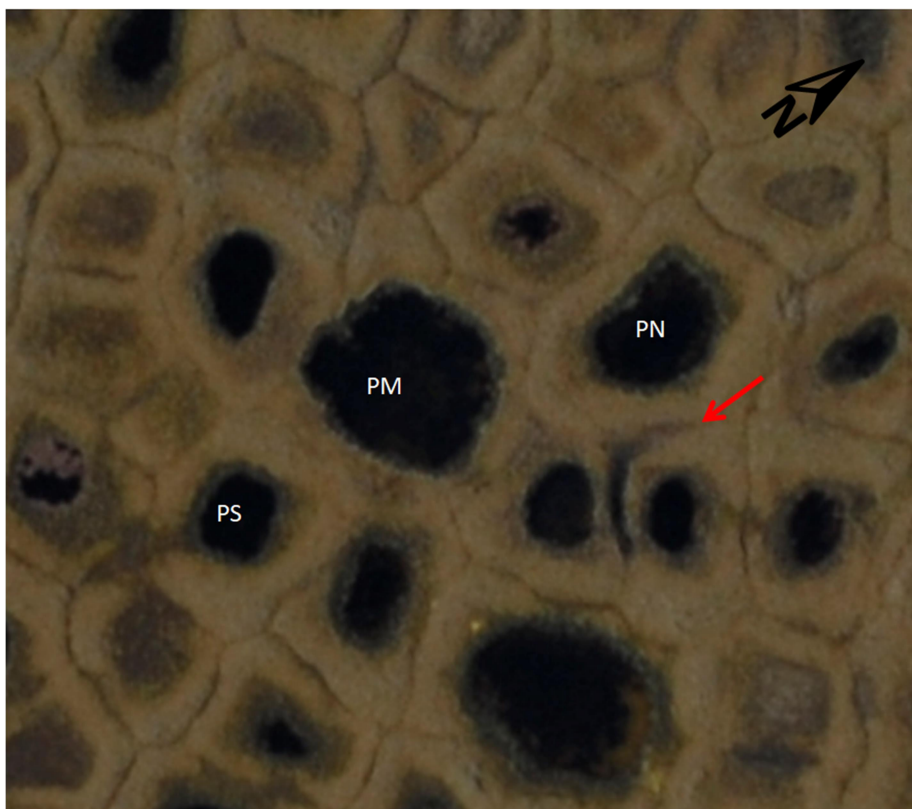
Figure 15: Satellite picture of the three sampled Polygons (PS = Polygon South, PM = Polygon Middle, PN = Polygon North) of Samoylov (changed after Boike 2014). The red Arrow marks a crescent-shaped waterbody, which may have an influence on Polygon North (PN).

Two DOC concentrations of polygons do not fit into this range. A higher concentration of 7.63 mg/L was measured in a sample from Polygon South in 2017. Ecological events and interactions could influence DOC concentrations in individual ponds, such as is seen in, the very high concentration of DOC in Polygon South in 2017. An algal bloom is an event that frequently occurs in ponds and lakes at different times during summer (personal communication Dr. Anne Morgenstern, Alfred-Wegner Institute, Potsdam 2019). Thus, the extreme peak in concentration is not a unique attribute to show a relationship

between the size of a waterbody and the concentration of DOC because it happens in small and bigger water bodies.

The lower concentration (3.7 mg/L) was found in a sample of Polygon North in 2017. A difference in the hydrogeological shape might be the reason for this change. Possible changes between the years could result in a degradation of the polygon or a new lateral in- /outflow. In a satellite image, taken in 2014 (Figure 15), no real evidence for a future in- / outflow or any change in shape, is visible for Polygon North. The only possible hint for a change of the hydrogeological shape can be the crescent-shaped waterbody (Figure 15: red arrow), which could nowadays be connected with the Polygon North. This could mean that due to freezing and thawing the degradation of the remaining soil, which divorces the Polygon North from the two smaller ponds in south-eastern direction and the crescent-shaped waterbody, took place. This connection would lead to a bigger surface area and a larger volume of this waterbody.

Other studies show similar results. In measurements of Abnizova et al. (2012) the concentration of DOC in polygons is higher too (Table 4). The concentration in lakes on the other hand is low. One of the lakes sampled in the study of Abnizova et al (2012) shows a deviant high concentration of DOC, which is explained by its connection with the floodplain of Samoylov. The floodplain supplies more organic matter to Lake 1, which leads to an increase of the DOC concentration. This influence of the floodplain on the lake can be recognized in the satellite pictures (Appendix 2). Furthermore, the increasing Cl^- and Na^+ Ions support an influence from the Lena River (Appendix 3).

Table 4:   DOC concentrations of Abnizova (2012)

Abnizova	Lake 1	Lake 2	Pond 1	Pond 2	Outlet	Floodplain
DOC (mg/L)	3.99	2.1	4.2	6.8	2.79	4.29
min (mg/L)	2.79	1.7	3.1	4.2	1.89	2.6
max (mg/L)	5.6	2.6	5.4	14.4	3.8	6.5

Since the general volume is smaller a higher concentration would automatically be assumed. This causality leads to the hypothesis that the concentration of DOC is higher in ponds than in lakes on islands from the first terrace.

The DOC concentration is not the only feature which is higher in polygons. Samples taken from these polygons show also a higher $\Delta^{14}C$ value > 0‰ indicative of a modern carbon source. While $\Delta^{14}C$ of 0‰ would reflect the atmospheric ^{14}C content of 1950, much higher radiocarbon levels were reached in the second half of the 20th century as a result of the nuclear bomb tests in the 1950s (Trumbore 2009). By comparing the measured $\Delta^{14}C$ values of the samples with the values of the atmosphere from the years 1955 to 2017, one can see that the signature of the polygons and the atmospheric values of 2002 are most similar (Table 5).

Table 5:   Delta ^{14}C values of the atmosphere of the northern Hemisphere (Graven et al. 2017)

Date	1999	2000	2001	2002	2003	2004	2005
Delta $^{14}CO_2$ [‰]	94.1	88.3	82.2	76.2	70.6	65.4	60.7

The active layer does not only derive from one special year, which makes it also inhomogenous in the $\Delta^{14}C$-signature. One has to consider this mixture of material from the year of sampling and the years before (Table 6). This would mean for the measurement from Polygon Middle of 56 ‰ $\Delta^{14}C$ in 2016 that a mixture of the same amount of material from the years 2016 to 2000 lead to the measured $\Delta^{14}C$ signature. The material dissolved in Polygon South with a $\Delta^{14}C$ of 50 ‰ results from the period 2016 to 2002. The lowest $\Delta^{14}C$ signature measured in Polygons in 2016 with 46 ‰ can be matched to period

from 2016 to 2004 result. The measurements of 2017 show Δ ^{14}C values of 54 ‰ and 60 ‰, which can be correlated to periods from 2017 to 1999 for 54 ‰ and 2017 to 1997 for 60 ‰ (Table 6).

Table 6:   Calculation of the origin of modern carbon

	2016 Polygon Middle	2016 Polygon South	2016 Polygon North	2017 Polygon South	2017 Polygon Middle
Measured in Sample	56 ‰	50 ‰	46 ‰	60 ‰	54 ‰
Calculated average	56,54	51,32	46,41	61,14	55,81
	=	=	=	=	=
1997	-	-	-	103,1	-
1998	-	-	-	99,2	-
1999	-	-	-	94,1	94,1
2000	88,3	-	-	88,3	88,3
2001	82,2	-	-	82,2	82,2
2002	76,2	76,2	-	76,2	76,2
2003	70,6	70,6	-	70,6	70,6
2004	65,4	65,4	65,4	65,4	65,4
2005	60,7	60,7	60,7	60,7	60,7
2006	56,6	56,6	56,6	56,6	56,6
2007	52,9	52,9	52,9	52,9	52,9
2008	49,4	49,4	49,4	49,4	49,4
2009	45,8	45,8	45,8	45,8	45,8
2010	41,6	41,6	41,6	41,6	41,6
2011	37,3	37,3	37,3	37,3	37,3
2012	30,4	30,4	30,4	30,4	30,4
2013	24,3	24,3	24,3	24,3	24,3
2014	19,6	19,6	19,6	19,6	19,6
2015	13,8	13,8	13,8	13,8	13,8
2016	8	8	8	8	8
2017	-	-	-	8	8

Since the Δ^{14}C values of DOC are higher than the contemporaneous atmosphere, there is no indication of admixture of fossil carbon to DOC. However, as organic matter synthesized during the last 60 years contains significantly high ^{14}C levels, a possible contribution of older carbon could be masked. It is not possible to calculate the distribution of old carbon with simultaneous consideration of the enrichment of ^{14}C, because the signature of the most enriched carbon is unknown. Therefore carbon, which is dissolved in the ponds could also have been released by sources older than 12 to 20 years and covered by the enriched material. A mix with a high enriched Δ^{14}C would also explain the much higher concentration in ponds.

In 2017, even the Δ^{14}C-signature of Polygon North decreased to values similar to those of North Lake, North Lake Outflow, Floodplain and Outflow at the coast. This signature represents a mix of the modern organic production with carbon captured by plants from the atmosphere and a small amount of possibly older carbon from other sources. In Figure 15 a possible change of the hydrogeological shape is depicted. The increase in volume resulting from the changed hydrogeological shape, could lead to a talik, which can reach deeper layers than the other ponds. Those deeper layers might add groundwater to the pond. This would lead to a more depleted Δ^{14}C-signature.

Lakes like the North Lake reach deeper layers, because of their size and volume. Groundwater with old organic carbon can reach the lakes easily and make the Δ^{14}C-signature decrease (Figure 13). The Δ^{14}C-signature differs between ponds influenced by leached out material from the last 12 to 20 or even older years and bigger lakes like the North Lake influenced by modern production by microorganisms resulting in a small depletion by older organic carbon.

Taking these aspects into consideration, it seems that there is a relationship between the size of a waterbody and the concentration of DOC and its Δ^{14}C-signature. Larger waterbodies have a lower concentration and a contemporaneous signature resulting from modern production and a possible influence of older Carbon. Barnes et al. (2018) support the hypothesis of a relationship between the size of waterbodies, the concentration of DOC and the Δ^{14}C-signature. They recognized that in shallow flow paths, which can be represented by ponds, the concentration increases and the Δ^{14}C-signature of DOC is modern (>0‰). Contrariwise, deeper flow paths show a lower DOC concentration and more depleted Δ^{14}C-signatures, which can be compared to deeper waterbodies like lakes (Figure 16).
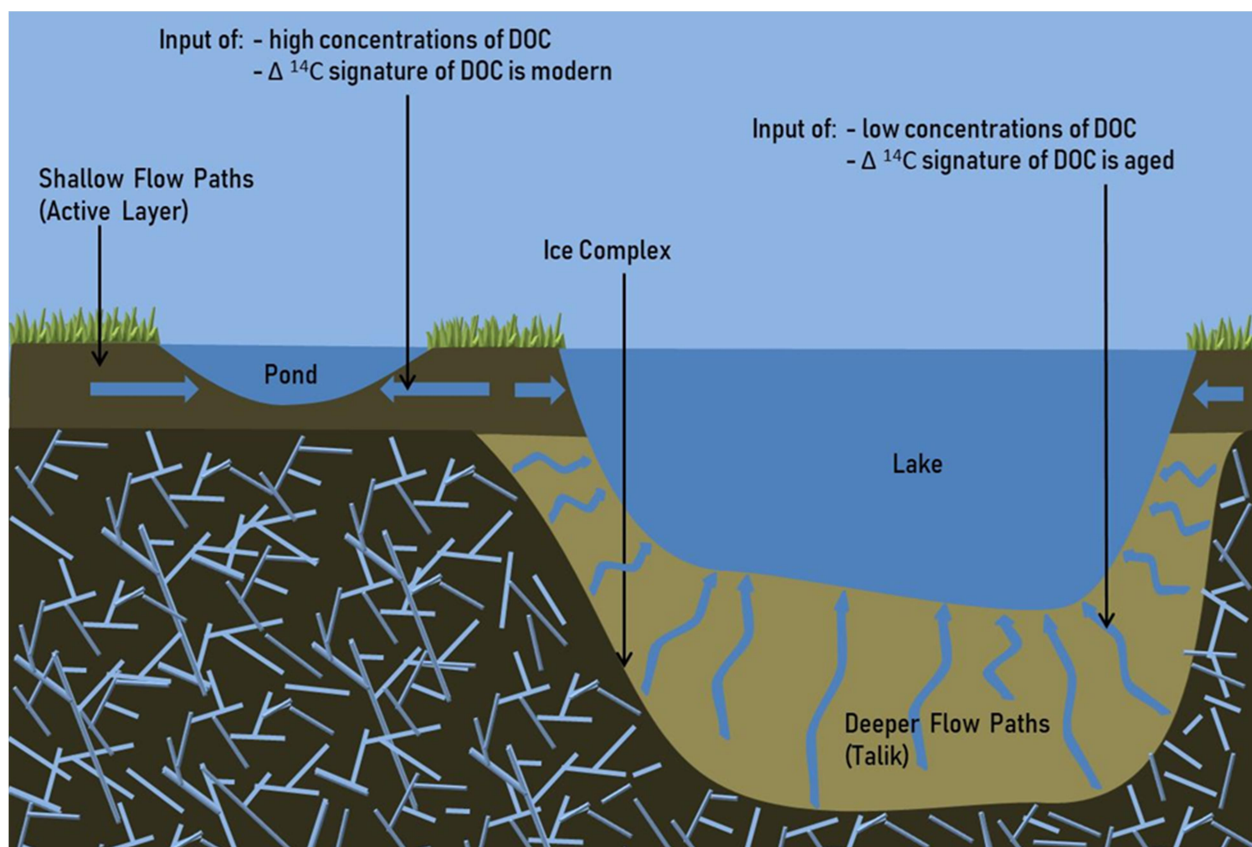
Figure 16: Conceptual model to show the impact of Shallow flows through active Layers on ponds and deeper flows through Taliks in lakes (compare with Barnes et al. 2018)

The named features consequently show that polygons mainly have a high concentration with an enriched signature and larger water bodies a lower concentration and a signature of recent production. This leads to the next paragraph questioning what happens to this carbon.

6.2   Calculation for the ratio of old Carbon

For the calculation of the ratio between old and modern carbon I used the information of Graven et al. (2017) and presumed a rough average of her atmospheric measurements of 2016 and 2017 (Δ^{14}C = 8‰) for the modern value. For the old carbon, I used the oldest stratigraphic conventional ages from Krebtschek (2002) for Kurungnakh and Kuptsov (1996) for Samoylov. A conventional age can be determined with the help of the fraction modern carbon signature F^{14}C, which is the result of a measurement

by an AMS. If the $F^{14}C$ is depleted in contrast to the atmospheric signature from 1950, one can calculate with the following equation the conventional age before present (before 1950(BP)):

$$A(conventional\ radiocarbon\ age) = ln(\frac{F\ ^{14}C}{-\lambda 14_C}) \tag{2}$$

$A(conventional\ radiocarbon\ age)$	The age of a sample calculated with the $F^{14}C$, which was measured by a AMS
$F14_C$	Fraction modern Carbon value
$-\lambda 14_C$	Half-life of ^{14}C (=(LN(2)/5568))

The converted equation:

$$F14_C = e^{A*-\lambda 14_c} \tag{3}$$

$A(conventional\ radiocarbon\ age)$	The age of a sample calculated with the $F^{14}C$, which was measured by MICADAS
$F14_C$	Fraction modern Carbon value
$-\lambda 14_C$	Half-life of ^{14}C (=(LN(2)/5568))

With equation (3) it was possible to calculate the $F^{14}C$ for the measured soil core samples from Krebtschek (2002) and Kuptsov (1996). To move on the $F^{14}C$ needed to be calculated into the $\Delta^{14}C$.

In equation (4) the $F^{14}C$ for the atmosphere in 2016 and 2017 is calculated with the $\Delta^{14}C$ Ingeborg Levin published on ICOS. $\Delta^{14}C$ shows the depletion and enrichment regarded to a normalized standard in per mil.

$$F14_C = \frac{\Delta 14_C}{1000*0,99169} + 1 \tag{4}$$

$F14_C$	Fraction modern Carbon value
$\Delta 14_C$	$\Delta^{14}C$ value
0,99169	Calculated by e^((1950-2019)/8267)

With the help of the calculated F14C it was possible to calculate the amount of old organic carbon in the samples. F14C allows isotope mass balance calculations according to the equations (5) and (6) (Wacker et al. 2010):

$$R_S = \frac{R_m*m_m-R_c*m_c}{m_m-m_c} \tag{5}$$

R_s	Fraction modern Carbon value of the sample
R_m	Fraction modern Carbon value of the measurement
R_c	Fraction modern Carbon value of the contaminant mass
m_m	Mass of the measurement
m_c	Mass of the contaminant mass

Rearrangement of the equation results in:

$$m_A = \frac{(R_m-R_S)*m_m}{(R_A-R_S)} \tag{6}$$

R_S	Fraction modern Carbon value of the Soil, in equation 4 R_s
R_A	Fraction modern Carbon value of the Atmosphere, in equation 4 R_c
R_m	Fraction modern Carbon value of the measurement
m_m	Mass of the measurement
m_A	Mass of the modern Carbon (Atmosphere) in equation 4 m_c

6.3 What happens to dissolved organic carbon in polygons and on the way to Lena River on Samoylov?

Ponds with a higher concentration of DOC are not connected to other waterbodies by surface channels. This causes a supersaturation of carbon in ponds, which leads to an emission of carbon to the atmosphere. Shirokova et al. (2013) recognized something similar during their studies. They found a correlation between aquatic CO_2 concentration and surface area. Water bodies with surface areas below 100 m^2 have a significant increase in dissolved CO_2 concentration with decreasing waterbody surface area. This means that in smaller ponds the CO_2 concentrations increases with decreasing water surface area. This observation could also explain the decrease in concentration, if the shape of Polygon North changed from the year 2016 to 2017 to a waterbody with a larger surface area.

Carbon which is leached into the larger water bodies may outgas shortly after entering the water. Algesten et al. (2004) detected, that 30 to 80 % of total organic carbon which entered freshwater bodies is lost in lakes due to mineralization and emission to the atmosphere. Abnizova et al. (2012) recognized that the outgassing of CO_2 is much higher than the lateral runoff. The concentration of modern DOC is possibly also higher, because microorganisms metabolize the older dissolved organic carbon. In a study from McCallister et al. (2012) the respiration of carbon by aquatic bacterioplankton was investigated. They recognized that the $\Delta^{14}C$ signature of respired CO_2 ranges from 94 to -172 ‰. This shows that carbon from a range of different sources is metabolized by bacteria. The newly produced DOC is transported downstream to the floodplain and the outflows and the dissolved carbon from the soil gasses out.

Along the flowpath of the water from North Lake to the floodplain and the outflow to the river Lena the $\Delta^{14}C$ signature does not change significantly (cp. Figure 13). The only change, which could be recognized, is an increase in concentration of DOC at the floodplain and the outflow at the coast.

The reason why $\Delta^{14}C$ signatures remain the same while the concentration increases, may have something to do with a higher modern production by plants and microorganisms on the floodplain (Figure 17). Flooding events and the outflows from thermokarst lakes located at the eastern plain of Samoylov deliver a lot of nutrients and carbon to the floodplain, which leads to a higher microbiological activity. According to this data the majority of the dissolved organic carbon seems to be the result of modern productions and a small amount of the enriched carbon sources from the last 60 years, which is transported into the river Lena.
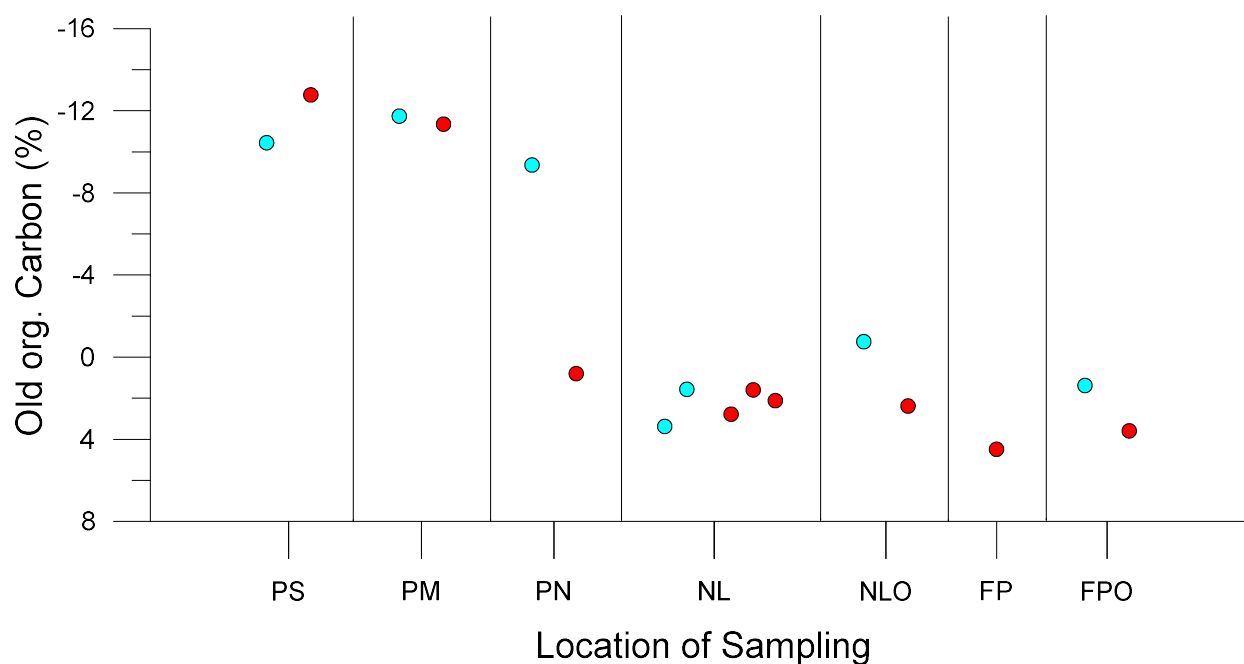
Figure 17: Percentage of old organic DOC on Samoylov (Samples from 2016 (turquoise); Samples from 2017 (red))

This emission of modern Δ^{14}C can be recognized in DOC measurements from Olga Ogneva. DOC, which has been analyzed by her results from water samples that have been filtered with a 0.7 µm filter (personal communication Olga Ogneva, Alfred-Wegener Institute, Bremerhaven 2019). The measured Δ^{14}C values look nearly like the ones from the polygons (Appendix 4 and Appendix 5).

6.4 What happens to particulate organic carbon on the way to Lena River on Samoylov?

The concentration of POC on Samoylov is generally lower than the DOC. This is linked to the low transport energy in the lakes and their small outflows. The decrease of POC concentration in North Lake and increase in the following samples (cp. Figure 13 b) from the year 2017 looks nearly like the decrease and later increase of DOC concentration (cp. Figure 13a). This would mean that the general distribution of carbon release is similar for DOC and POC at the same time and location.

However, the trend of 2016 shows a generally higher amount of POC and a large increase at North Lake Outflow. This increase of measured POC concentration is a result of heavy rainfalls. Between 11 am at the 1st of August and 2 am at the 2nd of August, 27.2 mm rainfall was measured at the meteorological station on Samoylov (Boike 2019). This heavy rainfall lead to erosion and mobilization of a lot of suspended load. This explains the extraordinary increase of the POC concentration at the Outflow of North Lake two days later. This rainfall event mainly caused the transport of suspended load from modern surface soil, which can be recognized by the Δ^{14}C signature of North Lake Outflow. This signature looks like the Δ^{14}C signatures of DOC from North Lake and its Outflow (cp. Figure 13 c). With a value of 6.2‰, the Δ^{14}C value of the DOC is a little bit lower than the 8‰ of the atmosphere in 2016 and 2017. This could lead to the fact that mostly recent produced organic carbon and older organic carbon, which is depleted in ^{14}C lead to the 6.2‰. The percentage of old organic carbon is 0.3% for North Lake Outflow, which explains the only slightly lower ^{14}C signature (Figure 18).
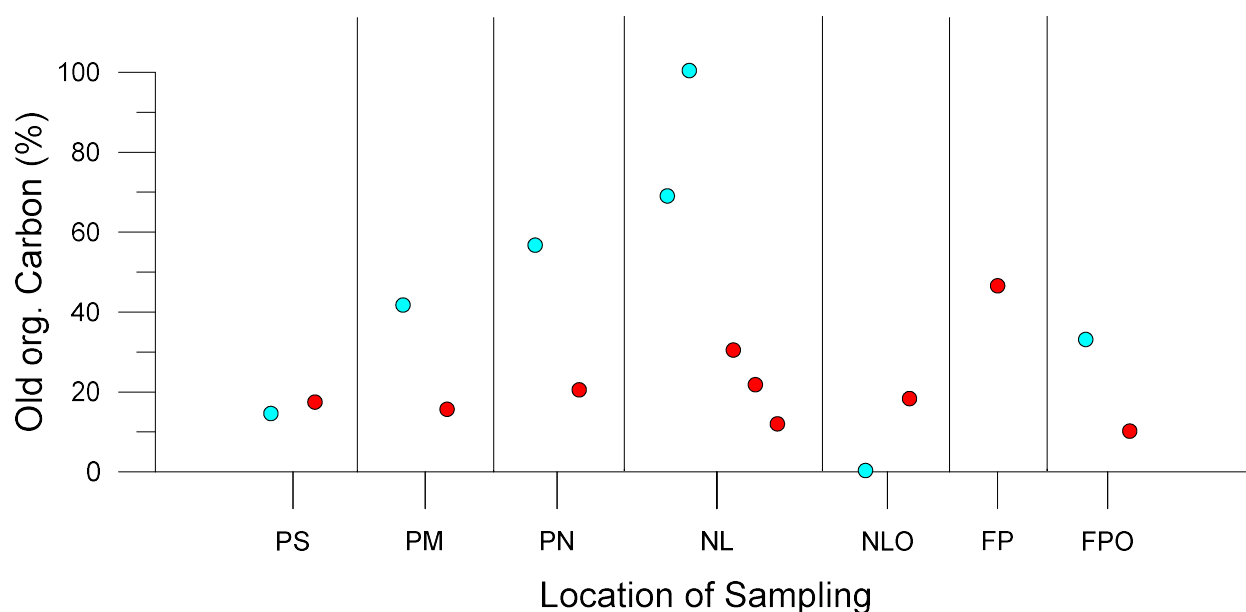
Figure 18: Percentage of old Carbon on Samoylov (Samples from 2016 (turquoise); Samples from 2017 (red))

POC from 2016, which was sampled in the Polygons and the North Lake, is much older than those from 2017. The reason for this could be the later sampling in August. The soil has a higher temperature in August 2016 than in July 2017. Therefore, more old organic material can be mobilized (Figure 18). The heavy rain event and wind speeds from 22.57 km/h to 35.2 km/h (Boike 2019) could have caused turbulent movements in the waterbodies, which lead to swirling of stratified suspended load (bagger) and POC from the ground into the water column.

These results show that during summertime, only a small amount of POC is transported down the Outflows to the floodplain and the Lena River. Nevertheless, during certain events like snowmelt, possible floods, heavy rainfalls and storms large amounts of POC can be mobilized and transported from the island to the river.

6.5   What happens to dissolved organic carbon on the way to the Lena River on Kurungnakh?

Kurugnakh island is composed of Pleistocene age deposits to a large extent and belongs to the Third Terrace unit of the Lena Delta. The concentration and the age of DOC increase from Oval Lake to Lucky Lake in both years. Lucky Lake is larger than Oval Lake. The question arises whether the size of the lake has an impact on the concentration of DOC. A relationship between the larger Lucky Lake and a higher concentration would disprove the hypothesis, which was proposed for the waterbodies on Samoylov stating that smaller waterbodies have a higher concentration than larger waterbodies.

Lucky Lake is larger than the Oval Lake, but has a higher concentration of DOC. Lucky Lake has two inflows, which are directly fed by the Yedoma Ice Complex. Although no samples were analyzed in the framework of this thesis, data of Polakowskis (2015) were available (Figure 19). Both of the inflows have a much higher concentration than the inflow from Oval Lake to Lucky Lake and the Lucky Lake itself. However, the discharge of those inflows is very low (personal communication Dr. Anne Morgenstern, Alfred-Wegener Institute, Potsdam 2019).

Another important influence on the increasing DOC concentration of the lake is that erosion occurs along the north shore of this waterbody (Figure 19). Through this erosion, old organic material, which is stored in the Yedoma Ice complex, is supplied directly into the lake. This is probably the reason for a higher concentration in Lucky Lake and also a more depleted Δ^{14}C-signature.

The next bigger change of DOC concentration and Δ^{14}C-signature occurs between the samples of Lucky Lake and the Outflow at the coast. The DOC concentration and Δ^{14}C-signature develop from Lucky Lake center over the following samples towards the outflow at the coast to a negative trend in concentration and a younger ongoing Δ^{14}C-signature. It seems like the closer the samples were taken towards the stream, the more, older DOC is metabolized and the signature becomes younger. In addition, the lower the concentration of DOC gets, the younger the signature becomes (cp. Figure 14). This could mean that old organic carbon is leaving the system along the flow from Lucky Lake towards the outflow on Kurung-nakh.

The samples taken from Lucky Lake center, close to the Lucky Lake outflow and directly at Lucky Lake Outflow also depict a trend of decreasing DOC concentration and increasing Δ^{14}C-signature. One possible reason for a decrease of concentration is the metabolism by microorganisms which would be an explanation for the increase of the Δ^{14}C-signature as well. Ancient organic Carbon, which is stored in frozen soils, is quite instable, which makes it easy for microorganisms to metabolize (Mann et al. 2015). During expeditions to Kurungnakh carpets of algae and bacteria could be recognized in the mainstream (personal communication Dr. Anne Morgenstern, Alfred-Wegener Institute, Potsdam 2019). Spencer et al. (2015) show similar findings. They recognized a loss of 50% of DOC in less the 7 days due to a rapidly utilization by microbes. In addition to a possible metabolism by microorganisms, instable DOC can be mineralized by UV-radiation (Corin et al. 1996). It remains to be answered whether the connection between concentrations and the Δ^{14}C-signature proves a possible metabolism and mineralization of old carbon on the way from Lucky Lake to the Outflow at the coast.

The samples which have been analyzed for this work do not cover the entire flowpath from Lucky Lake Outflow towards the outlet at the coast, but data from Polakowski (2015) can complete the overview of the stream and other inflows to it. Following the lines along the outflow (Figure 19), a decrease of concentration at each of the inflows is recognizable (Figure 20). Metabolism and mineralization of old carbon would explain a possible decrease in concentration on the way from Lucky Lake to the outlet at the coast. The inflows towards the stream are bearing water, which has been released from sediments of the first terrace of Kurungnakh and lead to dilution. The only inflow which has a higher concentration than the main stream is fed by a lake close before the outlet. Notable about the DOC concentrations of Polakonwski (2015) is that the outlet nearly has a higher concentration as the Lucky Lake itself.
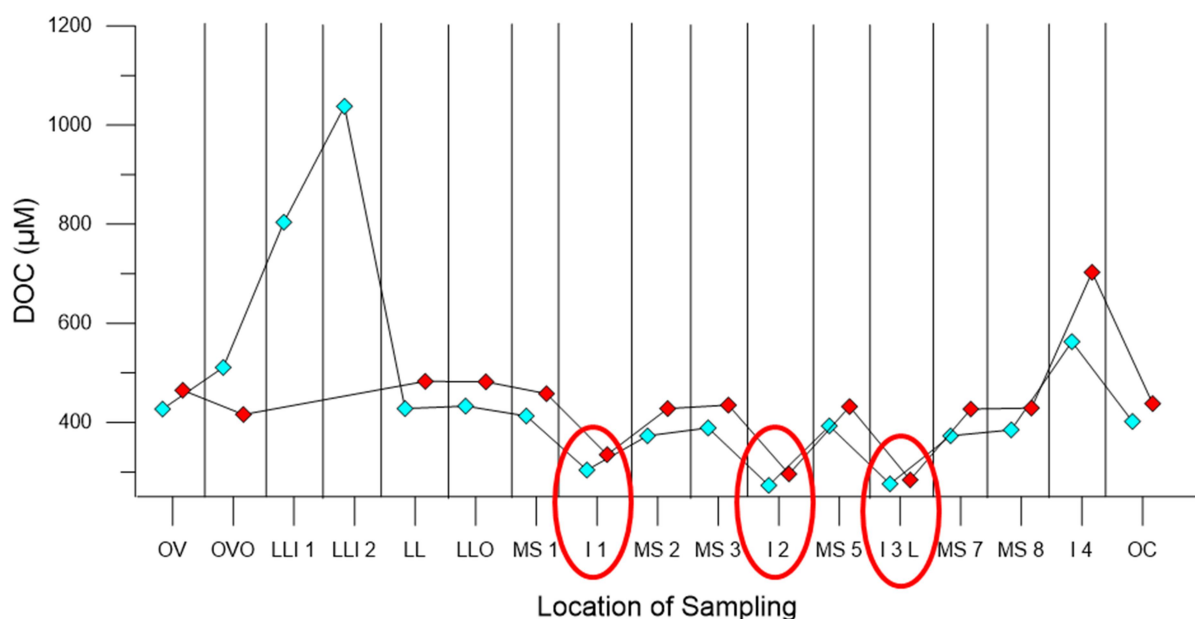
Figure 19: DOC concentrations from 2013 (turquoise) and 2014 (red) on Kurungnakh from Oval Lake to the out-flow at the coast (Data from Polakowski (2015) (DOC samples were taken with 0,75 µm Filters))
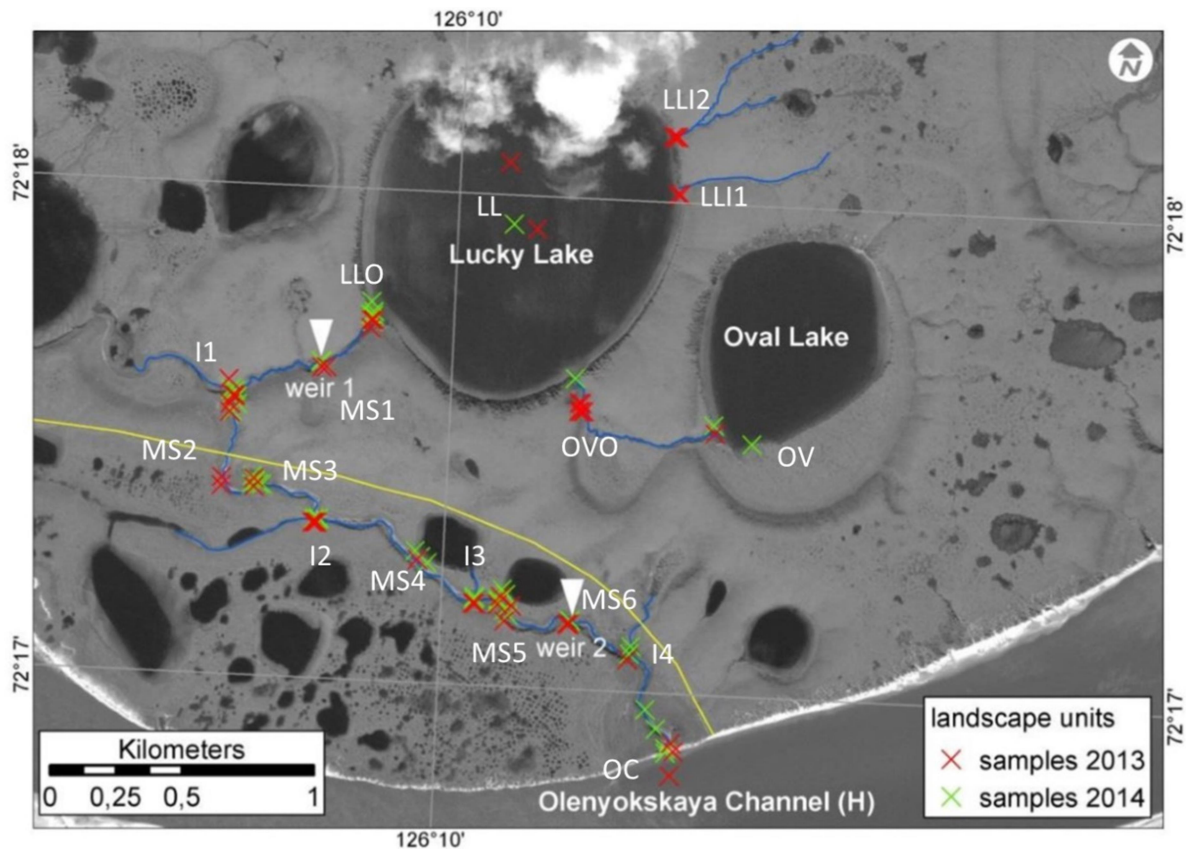
Figure 20: Sampling locations of Polakowski (2015) (changed after Polakowski (2015))

To decide if the data represents a dilution or possible outgassing the following calculations need to be done.

For a calculation of a possible loss of DOC due to outgassing, the discharge measurements and DOC concentrations of Lydia Polakowski (2015) were used (Table 7).

Table 7: DOC measurements on Kurungnakh from 2013 (Polakowski (2015))

Location	DOC conc. [mg/L]
Weir 1	4.96
Inflow (I1)	3.65
Mainstream (MS2)	4.48

Three different inflows can be recognized in Figure 20 between the discharge weir 1 and discharge weir 2. Assuming that every inflow adds the same amount of water to the stream and that no other in- or outflows exist at this stream the following calculation can be made (Table 8).

Table 8: Flow rates and estimated discharge values after the consideration of equal strong inflows (measurements after Polakowski (2015))

Location	Discharge value [m³/d] minima	Discharge value [m³/d] maxima
Weir 1	200	1700
Weir 2	500	3000
Weir 2 - Weir 1	300	1300
Inflow 1 = 1/3 Weir 2 - Weir 1	100	433
Mainstream (MS2) = Weir 1 + Inflow 1	300	2133

The subsequent calculations will focus on the relation of discharge and mass of DOC per day. If all of the water, which runs off **per day** at weir one and the inflow, results in the Mainstream, then the discharge per day at point MS2 should be the total of both.

$$Q_{Weir\ 1} + Q_{Inflow\ (I1)} = Q_{Mainstream\ (MS2)} \tag{7}$$

$Q_{Weir\ 1}$	Discharge at Weir 1 [m³/d]
$Q_{Inflow\ (I1)}$	Discharge at Inflow 1 [m³/d]
$Q_{Mainstream\ (MS\ )}$	Discharge at Mainstream (MS2) [m³/d]

If the dissolved Carbon in this water is transported down the flow without any loss, the mass of weir 1 and the inflow should give the total measured DOC at MS2.

$$m_{(DOC)Weir\ 1} + m_{(DOC)Inflow\ (I1)} = m_{(DOC)Mainstream\ (MS2)} \tag{8}$$

$m_{(DOC)Weir\ 1}$	Transported mass of DOC at Weir 1 [g/d]
$m_{(DOC)Inflow\ (I1)}$	Transported mass of DOC at Inflow (I1) [g/d]
$m_{(DOC)Mainstream\ (MS2)}$	Transported mass of DOC at Mainstream (MS2) [g/d]

The calculated DOC masses should be the same as the measurement if there is no loss of DOC on the way from weir 1 to MS2. Due to the consideration of no other in- or outflows at the surface as well as underground flows, the only way to lose DOC is outgassing in the atmosphere. To prove a possible loss of DOC, the following equation is used to calculate the mass of dissolved Carbon in Mainstream MS2 with the concentrations and flow rates of weir 1 and the inflow I1.

$$Q_{Weir\ 1} * c_{Weir\ 1} + Q_{Inflow\ (I1)} * c_{Inflow\ (I1)} = m_{(DOC)Mainstream\ M2\ calculated} \tag{9}$$

$Q_{Weir\ 1}$	Discharge at Weir 1 [m³/d]
$Q_{Inflow\ (I1)}$	Discharge at Inflow 1 [m³/d]
$c_{Weir\ 1}$	Concentration of DOC at Weir 1 [mg/L]
$c_{Inflow\ (I1)}$	Concentration of DOC at Inflow (I1) [mg/L]
$m_{(DOC)Mainstream\ (MS2)calculated}$	Transported mass of DOC at Mainstream (MS2) [g/d]

The following equation is used to calculate the mass of dissolved Carbon in Mainstream M2 with the considered flow rate at M2 and the measured concentration of DOC at this sampling point.

$$Q_{Mainstream\ MS2} * c_{Mainstream\ MS2} = m_{(DOC)Mainstream\ MS2\ calculated} \qquad (10)$$

$Q_{Mainstream\ (MS2)}$	Discharge at Mainstream (MS2) [m³/d]
$c_{Mainstream\ (MS2)}$	Concentration of DOC at Weir 1 [mg/L]
$m_{(DOC)\ Mainstream\ MS2\ calculated}$	Calculated transported mass of DOC at Mainstream (MS2) [g/d]

If the calculated mass of dissolved Carbon of equation 9 is higher than the one of equation 11 then DOC is released on the way from weir 1 to MS2.

$$m_{(DOC)Mainstream\ MS2\ calculated} - m_{(DOC)measured\ at\ Mainstream\ MS2} = m_{(DOC)outgassed} \qquad (11)$$

$m_{(DOC)\ Mainstream\ MS2\ calculated}$	Calculated transported mass of DOC at Mainstream (MS2) [g/d]
$m_{(DOC)measured\ at\ Mainstream\ MS2}$	Measured transported mass of DOC at Mainstream (MS2) [g/d]
$m_{(DOC)outgassed}$	Mass of outgassed DOC from Weir 1 to Mainstream (MS2) [g/d]

The calculations of both discharge measurements show a loss of DOC (Table 9).

Table 9: Mass of outgassed carbon (per day) for the minima and maxima discharge measurement

m	**(DOC)**	outgassed	13 g carbon
for minimal discharge			
m	**(DOC)**	outgassed	371.3 g carbon
for maximal discharge			

Whereas the Volume between maximum and minimum discharge is 7 times higher, the mass of outgassed carbon multiplies by a factor of 28. Because of the consideration of no further in- or outflow, the DOC can only be released due to outgassing. Either mineralization or metabolism as suggested in Spencer et al. (2015) and Mann et al. (2015) might be a possible way to mobilize the dissolved organic Carbon as CO_2. The connection between decreasing concentration and increasing $\Delta^{14}C$ signature can be explained with the calculated outgassing. The decrease in DOC concentrations after inflows might still be caused by a mix of metabolism and dilution from inflows.

The DOC, which reaches the Lena still has a $\Delta^{14}C$ signature of -289‰.

6.6 What happens to particulate organic carbon on the way to river Lena on Kurungnakh?

Comparable to Samoylov and the Arctic rivers (Wild et al. 2019), the concentration of POC is a lot lower than the concentration of DOC on Kurungnakh. A smaller increase is found at Lucky Lake in the year 2017, which could be caused by slumps from the surrounding soil into the lake. A much more significant increase in concentration is found at the outflow to the Lena River. The filter, which has been used to filter the water sample there, was completely covered with a thick dark layer of organic material. The two measurements at the outlet were taken from the same filter with different cutting sizes and show strongly varying results. This could be explained by the inhomogeneous structure of the organic layer. Beyond that high increase in concentration, those two filter samples show the most depleted $\Delta^{14}C$ signature. Due to rainfall starting on the 18th of August at 10 am until 9 am on the next day (2,8mm) more POC could be mobilized and a bigger slump could slide into Lucky Lake and other inflows from the third terrace. The particles did not have enough time to settle down in Lucky Lake. This is consistent with the fact that the second oldest signature was measured in a surface sample there. Because of continuous streams those particles are transported down the main stream at the surface of the flow. One could

assume that they do not settle down into the sediment of the stream, because the flow energy does not decrease. Reaching the outflow at the coast the transport energy is so high that it causes a washout of all arriving particles into the river (Table 7 and 8). Following the theory of Hjulström and Sundborg (1962) the mass of DOC (Table 7), which more easily carried by low energy currents, is higher than the mass of POC (Table 8).

Table 7: Calculated discharge of the maximum and minimum amount of transported DOC

	Weir 1 2016	Weir 1 2017	Weir 2 2017
Highest discharge	7874,4 g/d	8445,6 g/d	12636 g/d
	91,1 mg/s	97,8 mg/s	146,3 mg/s
Lowest discharge	926,4 g/d	993,6 g/d	2106 g/d
	10,7 mg/s	11,5 mg /s	24,4 mg/s

Table 8: Calculated discharge of the maximum and minimum amount of transported POC. 1/4 and 1/8 represents the cut size of the filters

	Weir 1 2016	Weir 1 2017	Weir 2 2017 1/4	Weir 2 2017 1/8
Highest discharge	699,72 g/d	475,32 g/d	21899 g/d	40320 g/d
	8,1 mg/s	5,5 mg/s	253 mg/s	466,7 mg/s
Lowest discharge	82,3 g/d	55,92 g/d	3649,8 g/d	6720 g/d
	0,95 mg/s	0,65 mg/s	42,2 mg/s	77,8 mg/s

The faster the stream becomes the more it washes down into the Lena. This observation supports the possible theory that POC can settle down in the lake sediments if the currents have too little energy to transport the particles. Particles which are released at the Yedoma Ice Complex and flow down into lakes can be stored in those lakes if the streams have low energy currents.

6.7 Why is DOC in Arctic rivers so young if the rivers are flowing through soils, which store old carbon from thousands of years?

After the results of the previous paragraphs, the question why the signature of the Arctic rivers is so young can be answered.

On the one hand DOC on Samoylov, which has been transported by lateral runoff, shows a modern signature. It mainly results from modern production. On Samoylov, the carbon, which is leached in Polygons results from the time when the atmosphere has been enriched by ^{14}C resulting of nuclear bombing tests (Trumbore 2009).

On the other hand, DOC which leaves the streams of Kurungnakh to the Lena has a low Δ^{14}C of -289‰. On Kurungnakh, the carbon, which is leached in lakes is older than that.

Only according to the Δ^{14}C-signature of those two islands the above stated question cannot clearly be answered. For this problem, it is important to remember the geology of the Delta. The Delta is divided in sediments from the first, second and third terrace. The first terrace sediments clearly make up the majority or the Delta. The first terrace is made up of fluvial sediments from the river. If the majority of islands like Samoylov draw down water from enriched ^{14}C accumulations, the water gets a ^{14}C-enriched amount of carbon.

Signature measurements by Wild et al. (2019) of the arctic rivers (Ob, Yenisei, **Lena** and Kolyma) showed average values of 72 ± 39 ‰, similar to Δ^{14}C-values of the DOC samples on Samoylov found in this study. In addition to the stronger influence by carbon from the first terrace islands than from the third terrace,

ancient DOC (younger than 20,000 BP) has a decay rate of 0.12 to 0.19 % per day and microbes utilize 50% of DOC in the first 7 days (Spencer et al. 2015).

The carbon in the Arctic rivers therefore looks so young, because, at the moment, the main component of entering carbon result from enriched sources and the smaller amount of released ancient DOC decays so fast that the enriched amounts to cover the small amounts of ancient DOC. According to the findings of Spencer et al. 2015, the majority of old DOC might outgas.

6.8   Which differences can be recognized between the different years of sampling?

One of the main differences is that the 2016 samples were taken in August while the samples from 2017 were taken in July. That may have an influence on the enriched and depleted Δ^{14}C-signatures of the years. As seen in a direct comparison of the samples from Polygon South and Middle, the POC samples of August 2016 have a more depleted Δ^{14}C signature, whereas DOC samples from July 2017 show modern enriched Δ^{14}C signatures (cp. Table 6). This might be caused by the fact that the thawing process is further progressed in August compared to July. This difference can also be recognized in the samples of DOC from Kurungnakh, but it is far less prevalent than for the POC samples.

In addition to the advanced thawing process, during the sampling in August 2016 heavy rainfalls with wind speeds of 22.57 km/h to 35.2 km/h (Boike 2019) caused a higher release of POC into waterbodies on Samoylov.

On the other hand, certain events were only present during the sampling in 2017. An algal bloom, probably led to an increase of DOC concentration in Polygon South in July 2017. In addition the hydrogeological shape, Polygon North might have changed due to degradation or freezing and thawing processes from 2016 to 2017. This change in shape might concern the surface area, volume and reaching depth.

7 Conclusiones

The results of this thesis show high concentrations of dissolved organic carbon are released to lakes and ponds ultimately into the Delta Lena. On Samoylov, which represents the first terrace unit, as well as Kurungnakh, which represents the third terraces unit, DOC is leached out of permafrost deposits. Differences in $\Delta^{14}C$ signatures help to better understand the carbon cycle in this region. To sum up all discussed results, the questions from the beginning will be answered in the following chapter one by one.

Beginning with the first question: Does a Relationship exist between the size of a waterbody, the concentration of old organic carbon and the $\Delta^{14}C$ signature?

With a preliminary evaluation of the data, it would seem that the samples collected on the two islands contradict each other. On Samoylov the larger analyzed water bodies had a lower concentration in DOC and POC than the smaller ponds. In contrast, on Kurungnakh the concentration was higher in the largest analyzed lake (Lucky Lake) and lower in smaller lakes, streams and outflows.

After taking a closer look at the data and the literature, those trends could be explained in different ways. The possible explanation for a higher concentration of DOC in ponds and the more modern $\Delta^{14}C$-signature can be the result of fast dissolution of soil into a small volume of water. The lakes on Samoylov have a lower concentration and a $\Delta^{14}C$-signature similar to the contemporaneous atmosphere, because leached DOC is metabolized and mineralized faster in a bigger lake. This hypothesis needs further analyses to be proved but provides a reasonable interpretation of the presented data. Additionally, more dissolved organic carbon seems to have a higher influence on waterbodies with a lower volume and depth. The same relation might be present on Kurungnakh too, but the samples for this study result from a draining smaller lake and a bigger lake, which erodes the old Yedoma Ice Complex at its surrounding, which leads to higher concentrations. Samples from smaller lakes without special properties on Kurungnakh might provide the same pattern.

Continuing with the second question: What happens to DOC and POC after it is solved from frozen soils? On Samoylov it seems as the concentration of DOC and POC increases the closer the flow comes to the outflow to the Lena. This is related to the floodplain and other outflows of lakes, which have an influence with their organic material. In addition a lot of modern new produced carbon is transported to the Lena. The older carbon might leave the system before due to mineralization, metabolism and outgassing. Events like floods, heavy rainfalls, and the melting at the beginning of the summertime lead to the mobilization of large amounts of old and modern POC to the Lena.

On Kurungnakh the DOC and POC have a much older $\Delta^{14}C$-signature released from the older sediments from the third terrace. POC is like on Samoylov mobilized by bigger events (floods, heavy rainfalls, melting of huge amounts of ice in the early summer). On Kurungnakh another event also occurs. Due to erosional processes of the slopes of the Yedoma Ice Complex a lot of old carbon is added to the waterbodies and the flows. Large amounts of carbon are mobilized to the outflow at the coast by high energy events and feed the Lena River.

By looking at the loss in concentration of DOC and the increasing $\Delta^{14}C$-signature, it at first appears as if there is a bigger release of CO_2 due to metabolism or mineralization of solved organic material. For the measurements between outflow of Lucky Lake and outflow at the coast, Lydia Polakowski's measurements could give a hint at dilution caused by inflows. The further calculation of carbon mass in the mainstream with some considerations, showed possible outgassing processes. Additionally, measurements from Lucky Lake center and the outflow of Lucky Lake support the theory of mineralization of fragile old org. components. These findings increasingly support a general loss of DOC due to outgassing.

The last issue which can partly be explained in this thesis concerns the question why the DOC in arctic rivers is so young even though the rivers are flowing through soils, which store thousands year old carbon. This question can only be partly answered because one study is not enough clarify an issue which is influenced by many divergent factors.

The Lena Delta is dominated by islands from the first terrace. Those islands are represented in this work by the samples from Samoylov. DOC, which reaches the river channel from Samoylov was mainly modern. Additionally, samples which were taken in ponds of this island showed strongly enriched Δ^{14}C-signatures. These can cover the depleted signatures of old Carbon which enters the Lena at one of the fewer islands from the third terrace, like Kurungnakh. On top of this, other researches recognized that ancient carbon decays very fast upon entering the waterbodies and rivers (Mann et al. 2015; (Spencer et al. 2015).

The recurring result of this work is that a large amount of ancient DOC decays or outgasses before it reaches the river. The enriched material from the last 60 years and the results of modern production dominate the input of DOC to the Lena River.

8   Outlook

To achieve a profound understanding of the processes of carbon release and loss further studies could not only lead to a better understanding but they could also support the stated thesis better.

CO_2 measurements like the ones being done by McCallister (2012) on lakes in Quebec, Canada could support and prove the thesis of mineralizing DOC in polygons and metabolism in lakes. Therefore these could show if the released CO_2 has an old Δ ^{14}C-signature.

On top of this, the decrease of DOC at the outflow from Kurungnakh to the Lena River proved in this thesis on the one hand and the increase of DOC at the outflow in Polakowski (2015) on the other hand remain another interesting inconsistency that is worth into looking further. Thorough analyses of this point regarding certain higher discharge events and the Δ ^{14}C-signatures of the inflows to Lucky Lake and the main stream, would enable a better understanding of the traveling of DOC and POC better.

With these additional studies and maybe even further water sampling on Samoylov, without heavy precipitation events, a better and clearer statement could be verified as an answer to this thesis.

9   References

Åberg, J., Bergström, A. K., Algesten, G., Söderback, K., & Jansson, M. (2004). A comparison of the carbon balances of a natural lake (L. Örträsket) and a hydroelectric reservoir (L. Skinnmuddselet) in northern Sweden. *Water Research*, *38*(3), 531-538.

Abnizova, A., Siemens, J., Langer, M., & Boike, J. (2012). Small ponds with major impact: The relevance of ponds and lakes in permafrost landscapes to carbon dioxide emissions. *Global Biogeochemical Cycles*, *26*(2).

Algesten, G., Sobek, S., Bergström, A. K., Ågren, A., Tranvik, L. J., & Jansson, M. (2004). Role of lakes for organic carbon cycling in the boreal zone. *Global change biology*, *10*(1), 141-147.

Are, F., & Reimnitz, E. (2000). An overview of the Lena River Delta setting: geology, tectonics, geomorphology, and hydrology. *Journal of Coastal Research*, 1083-1093.

Boike, J., Grüber, M., Langer, M., Piel, K., & Scheritz, M. (2012). Orthomosaic Samoylov Island, Lena Delta, Siberia, Bremerhaven, PANGAEA.

Boike, J., Kattenstroth, B., Abramova, E., Bornemann, N., Chetverova, A., Fedorova, I., ... & Langer, M. (2013). Baseline characteristics of climate, permafrost and land cover from a new permafrost observatory in the Lena River Delta, Siberia (1998-2011). *Biogeosciences (BG)*, *10*(3), 2105-2128.

Boike, J., Georgi, C., Kirilin, G., Muster, S., Abramova, K., Fedorova, I., ... & Langer, M. (2015). Physical processes of thermokarst lakes in the continuous permafrost zone of northern Siberia-observations and modeling (Lena River Delta, Siberia). *Biogeosciences Discussions*, *12*(15).

Boike, J., Nitzbon, J., Anders, K., Grigoriev, M., Bolshiyanov, D., Langer, M., ... & Wille, C. (2019). A 16-year record (2002–2017) of permafrost, active-layer, and meteorological conditions at the Samoylov Island Arctic permafrost research site, Lena River delta, northern Siberia: an opportunity to validate remote-sensing data and land surface, snow, and permafrost models. *Earth System Science Data*, *11*(1), 261-299.

Corin, N., Backlund, P., & Kulovaara, M. (1996). Degradation products formed during UV-irradiation of humic waters. *Chemosphere*, *33*(2), 245-255.

Duchemin, E., Lucotte, M., & Canuel, R. (1999). Comparison of static chamber and thin boundary layer equation methods for measuring greenhouse gas emissions from large water bodies §. *Environmental Science & Technology*, *33*(2), 350-357.

Fiedler, S., Wagner, D., Kutzbach, L., & Pfeiffer, E. M. (2004). Element redistribution along hydraulic and redox gradients of low-centered polygons, Lena Delta, Northern Siberia. *Soil Science Society of America Journal*, *68*(3), 1002-1011.

French, H.M. (2007): The periglacial environment. Third Edition, John Wiley & Sons,   Chichester.

Frey, K. E., & Smith, L. C. (2005). Amplified carbon release from vast West Siberian peatlands by 2100. *Geophysical Research Letters*, *32*(9).

Frey, K. E., & McClelland, J. W. (2009). Impacts of permafrost degradation on arctic river biogeochemistry. *Hydrological Processes: An International Journal*, *23*(1), 169-182.

Graven, H., Allison, C. E., Etheridge, D. M., Hammer, S., Keeling, R. F., Levin, I., ... & Vaughn, B. H. (2017). Compiled records of carbon isotopes in atmospheric CO2 for historical simulations in CMIP6. *Geoscientific Model Development (Online)*, *10*(12).

Grotheer, H. (2012): Radiocarbon signature of dissolved organic carbon (DOC) in arctic rivers - An evaluation of DOC extraction methods and a Lena Delta case study, Master thesis, Universität Bremen.

Harris, S. A., French, H. M., Heginbottom, J. A., Johnston, G. H., Ladanyi, B., Sego, D. C., & van Everdingen, R. O. (1988). Glossary of permafrost and related ground-ice. Terms National Research Council of Canada Ottawa, Ontario, Canada KIA OR6.

Hjulström, F., & Sundborg, Å. (1962). *The geomorphological laboratory*. na.

Holmes, R. M., McClelland, J. W., Peterson, B. J., Tank, S. E., Bulygina, E., Eglinton, T. I., ... & Staples, R. (2012). Seasonal and annual fluxes of nutrients and organic matter from large rivers to the Arctic Ocean and surrounding seas. *Estuaries and Coasts*, *35*(2), 369-382.

Jones, P. D., & Moberg, A. (2003). Hemispheric and large-scale surface air temperature variations: An extensive revision and an update to 2001. *Journal of climate*, *16*(2), 206-223.

Jonsson, A., Karlsson, J., & Jansson, M. (2003). Sources of carbon dioxide supersaturation in clearwater and humic lakes in northern Sweden. *Ecosystems*, *6*(3), 224-235.

Kirpotin, S., Polishchuk, Y., Bryksina, N., Sugaipova, A., Kouraev, A., Zakharova, E., ... & Dupre, B. (2011). West Siberian palsa peatlands: distribution, typology, cyclic development, present day climate-driven changes, seasonal hydrology and impact on CO2 cycle. *International journal of environmental studies*, *68*(5), 603-623.

Krbetschek, M. R., Gonser, G., & Schwamborn, G. (2002). Luminescence dating results of sediment sequences of the Lena Delta. *Polarforschung*, *70*, 83-88.

Kuptsov, V. M., & Lisitsin, A. P. (1996). Radiocarbon of Quaternary along shore and bottom deposits of the Lena and the Laptev Sea sediments. *Marine Chemistry*, *53*(3-4), 301-311.

Mann, P. J., Eglinton, T. I., McIntyre, C. P., Zimov, N., Davydova, A., Vonk, J. E., ... & Spencer, R. G. (2015). Utilization of ancient permafrost carbon in headwaters of Arctic fluvial networks. *Nature Communications*, *6*, 7856.

Morgenstern, A., Grosse, G., Günther, F., Fedorova, I., & Schirrmeister, L. (2011). Spatial analyses of thermokarst lakes and basins in Yedoma landscapes of the Lena Delta. *The Cryosphere Discussions*, *5*, 1495-1545.

Morgenstern, A., Ulrich, M., Günther, F., Roessler, S., Fedorova, I. V., Rudaya, N. A., ... & Schirrmeister, L. (2013). Evolution of thermokarst in East Siberian ice-rich permafrost: A case study. *Geomorphology*, *201*, 363-379.

McCallister, S. L., & del Giorgio, P. A. (2012). Evidence for the respiration of ancient terrestrial organic C in northern temperate lakes and streams. *Proceedings of the National Academy of Sciences*, *109*(42), 16963-16968.

McGuire, A. D., Anderson, L. G., Christensen, T. R., Dallimore, S., Guo, L., Hayes, D. J., ... & Roulet, N. (2009). Sensitivity of the carbon cycle in the Arctic to climate change. *Ecological Monographs*, *79*(4), 523-555.

Oechel, W. C., Hastings, S. J., Vourlrtis, G., Jenkins, M., Riechers, G., & Grulke, N. (1993). Recent change of Arctic tundra ecosystems from a net carbon dioxide sink to a source. *Nature*, *361*(6412), 520.

Polakowski, L. (2015). Summer surface water chemistry dynamics in different landscape units from Yedoma Ice Complex to the Lena River , Master thesis University Potsdam.

Pokrovsky, O. S., Shirokova, L. S., Kirpotin, S. N., Audry, S., Viers, J., & Dupré, B. (2011). Effect of permafrost thawing on organic carbon and trace element colloidal speciation in the thermokarst lakes of western Siberia. *Biogeosciences*, *8*(3), 565-583.

Riedel, T. (2016). Expedition report of the Lena Delta 2016 expedition, August period.

Romanovskii, N. N., & Hubberten, H. W. (2001). Results of permafrost modelling of the lowlands and shelf of the Laptev Sea region, Russia. *Permafrost and periglacial processes*, *12*(2), 191-202.

Romanovsky, V. E., Smith, S. L., & Christiansen, H. H. (2010). Permafrost thermal state in the polar Northern Hemisphere during the international polar year 2007–2009: a synthesis. *Permafrost and Periglacial processes*, *21*(2), 106-116.

Ruff, M., Szidat, S., Gäggeler, H. W., Suter, M., Synal, H. –A., & Wacker, L. (2010). Gaseous radiocarbon measurements of small samples. *Nuclear Instruments and Methods in Physics Research Section B,* 268, 790-794.

Schirrmeister, L., Grosse, G., Wetterich, S., Overduin, P. P., Strauss, J., Schuur, E. A., & Hubberten, H. W. (2011a). Fossil organic matter characteristics in permafrost deposits of the northeast Siberian Arctic. *Journal of Geophysical Research: Biogeosciences*, *116*(G2).

Schirrmeister, L., Kunitsky, V., Grosse, G., Wetterich, S., Meyer, H., Schwamborn, G., ... & Siegert, C. (2011b). Sedimentary characteristics and origin of the Late Pleistocene Ice Complex on north-east Siberian Arctic coastal lowlands and islands–A review. *Quaternary international*, *241*(1-2), 3-25.

Schuur, E. A., Abbott, B. W., Bowden, W. B., Brovkin, V., Camill, P., Canadell, J. G., ... & Crosby, B. T. (2013). Expert assessment of vulnerability of permafrost carbon to climate change. *Climatic Change*, *119*(2), 359-374.

Schwamborn, G., Rachold, V., & Grigoriev, M. N. (2002). Late Quaternary sedimentation history of the Lena Delta. *Quaternary international*, *89*(1), 119-134.

Shirokova, L. S., Pokrovsky, O. S., Kirpotin, S. N., Desmukh, C., Pokrovsky, B. G., Audry, S., & Viers, J. (2012). Biogeochemistry of organic carbon, CO 2, CH 4, and trace elements in thermokarst water bodies in discontinuous permafrost zones of Western Siberia. *Biogeochemistry*, *113*(1-3), 573-593.

Spencer, R. G., Mann, P. J., Dittmar, T., Eglinton, T. I., McIntyre, C., Holmes, R. M., ... & Stubbins, A. (2015). Detecting the signature of permafrost thaw in Arctic rivers. *Geophysical Research Letters*, *42*(8), 2830-2835.

Spitzy, A., & Leenheer, J. (1991). Dissolved organic carbon in rivers. *Biogeochemistry of major world rivers*, *42*.

Synal, H. A., Stocker, M., & Suter, M. (2007). MICADAS: a new compact radiocarbon AMS system. *Nuclear Instruments and Methods in Physics Research Section B: Beam Interactions with Materials and Atoms*, *259*(1), 7-13.

Tarnocai, C., Canadell, J. G., Schuur, E. A., Kuhry, P., Mazhitova, G., & Zimov, S. (2009). Soil organic carbon pools in the northern circumpolar permafrost region. *Global biogeochemical cycles*, *23*(2).

Vonk, J. E., Mann, P. J., Davydov, S., Davydova, A., Spencer, R. G., Schade, J., ... & Eglinton, T. I. (2013). High biolability of ancient permafrost carbon upon thaw. *Geophysical Research Letters*, *40*(11), 2689-2693.

Wacker, L., Christl, M., & Synal, H. A. (2010). Bats: a new tool for AMS data reduction. *Nuclear Instruments and Methods in Physics Research Section B: Beam Interactions with Materials and Atoms*, *268*(7-8), 976-979.

West, J. J., & Plug, L. J. (2008). Time-dependent morphology of thaw lakes and taliks in deep and shallow ground ice. *Journal of Geophysical Research: Earth Surface*, *113*(F1).

Wetterich, S., Kuzmina, S., Andreev, A. A., Kienast, F., Meyer, H., Schirrmeister, L., ... & Sierralta, M. (2008). Palaeoenvironmental dynamics inferred from late Quaternary permafrost deposits on Kurung-nakh Island, Lena Delta, northeast Siberia, Russia. *Quaternary Science Reviews*, *27*(15-16), 1523-1540.

Wild, B., Andersson, A., Bröder, L., Vonk, J., Hugelius, G., McClelland, J. W., ... & Gustafsson, Ö. (2019). Rivers across the Siberian Arctic unearth the patterns of carbon release from thawing permafrost. *Proceedings of the National Academy of Sciences*, *116*(21), 10280-10285.

Winterfeld, M., Grotheer, H., Mollenhauer, G. (2017). Quantification, isotopic and compositional analysis of dissolved and particulate carbon in the Lena and water bodies of its Delta.

Internet sources:

http://www.awi.de/forschung/geowissenschaften/marine-geochemie/micadas/technik.html (letzter Zugriff: 14.06.2019)

ICOS RI, 2019. ICOS ATC 14C Release, Jungfraujoch (10.0 m), 2016-01-04-2018-07-16, https://hdl.handle.net/11676/0yDrKllpdGVPtMsFIMSUEm1N

Appendix

Appendix 1: Table of used and measured samples; F^{14}C (measured values); F^{14}C cor (Blank corrected values); Δ^{14}C (Blank corrected).

Location	Conc. [mg/L]	Sample	F^{14}C	= + - (abs)	age (y)	F14C s cor	σF14C s	Δ14 C	σΔ14 C	Sam-ple
Samoylov; North Lake, center;	2.828	L16-01a-1a	0,9966	0,0078	27,18	1,002054	0,008	-6,27	8,0097	DOC
Samoylov; North Lake, center; 3,7m	2.839	L16-01b-1a	1,0028	0,0079	-22,12	1,009567	0,0083	1,18	8,2522	DOC
Samoylov; North Lake, outflow	3.288	L16-02-1a	1,0133	0,0078	-106,1	1,01921	0,0081	10,74	8,1002	DOC
Samoylov; North lake, Polygon-1	4.335	L16-03-1a	1,0485	0,0081	-380,2	1,054991	0,0084	46,22	8,3511	DOC
Samoylov; North Lake, Polygon-2	4.922	L16-04-1a	1,0580	0,0082	-452,8	1,064892	0,0084	56,04	8,4071	DOC
Samoylov; North Lake, Polygon-3	4.505	L16-05-1a	1,0524	0,0080	-410,1	1,059509	0,0083	50,7	8,2793	DOC
Kurung-nakh;Lucky Lake, center;	4.464	L16-09a-1a	0,6390	0,0059	3597	0,635626	0,0061	-370	6,1349	DOC
Kurung-nakh;Lucky Lake, center; 2m	4.788	L16-09b-1a	0,6249	0,0052	3777	0,620996	0,0054	-384	5,3622	DOC
Kurung-nakh;Lucky Lake, center; 3,5-3,7m	5.092	L16-09c-1a	0,6287	0,0050	3728	0,624827	0,0052	-380	5,2004	DOC
Kurung-nakh;Lucky Lake, 50 to 70 m before outflow	4.908	L16-10a-1a	0,6369	0,0054	3624	0,6333	0,0056	-372	5,6066	DOC

Location	Conc. [mg/L]	Sample	F^{14}C	= + - (abs)	age (y)	F14C s cor	σF14C s	Δ14C	σΔ14C	Sample
Kurung-nakh;Lucky Lake, 50 to 70 m before out flow	4.775	L16-10b-1a	0,6359	0,0056	3637	0,6323	0,0058	-373	5,7732	DOC
Kurung-nakh;Lucky Lake, 50 to 70 m before outflow	4.806	L16-10c-1a	0,6347	0,0054	3652	0,631209	0,0056	-374	5,6235	DOC
Kurung-nakh;Lucky Lake, outflow	4.631	L16-11-1a	0,6515	0,0058	3442	0,648399	0,006	-357	5,9807	DOC
Kurung-nakh;Lucky Lake, inflow	4.561	L16-12-1a	0,7022	0,0062	2840	0,70033	0,0064	-305	6,3823	DOC
Kurungnakh;Oval Lake, center	4.599	L16-13a-1a	0,6917	0,0062	2961	0,689572	0,0064	-316	6,4014	DOC
Kurungnakh;Oval Lake, center	4.614	L16-13b-1a	0,6865	0,0060	3021	0,684151	0,0062	-322	6,2151	DOC
Kurungnakh;Oval Lake, center	4.481	L16-13c-1a	0,6791	0,0059	3109	0,676495	0,0061	-329	6,1402	DOC
Samoylov; Flood Plain, outflow (North Lake study site)	5.840	L16-22-1a	1,0045	0,0085	-36,3	1,010344	0,0088	1,95	8,8016	DOC
Samoylov, North Lake outflow	2.758	L17-01-3B	1,0006	0,0095	-4,8	1,006188	0,0098	-2,17	9,7602	DOC
Samoylov, North Lake center; ~4m water depth at sampling location	2.688	L17-04-8b0m	0,9989	0,0096	8,65	1,004533	0,0099	-3,81	9,8779	DOC

Appendix 1: Prosecution of Appendix 1 (Table of used and measured samples; F^{14}C (measured values); F^{14}C cor (Blank corrected values); Δ^{14}C (Blank corrected).)

Location	Conc. [mg/L]	Sam-ple	F^{14}C	= + - (abs)	age (y)	F14C s cor	σF14C s	Δ14 C	σΔ14 C	Sam-ple
Samoylov, North Lake center; ~4m water depth at sampling location	2.622	L17-04-8b 1,5m	1,004 0	0,0080	-31,7 2	1,00945 7	0,0082	1,07	8,222 6	DOC
Samoylov, North Lake center; ~4m water depth at sampling location	2.755	L17-04-8b 3m	1,001 6	0,0078	-12,8 3	1,00727 5	0,008	-1,1	8,021 7	DOC
Samoylov Katya Lake (on flood-lplain downstram of North Lake)	4.309	L17-05-8b	0,992 1	0,0074	63,6 6	0,99742 4	0,0076	-10,9	7,595 1	DOC
Samoylov; Outflow floodplain to Lena, down-stream of Katya Lake	4.943	L17-06-8b	0,995 9	0,0077	32,9	1,00116	0,0079	-7,16	7,906 6	DOC
Samoylov; Polygon pond North	3.712	L17-10-8b	1,006 2	0,0077	-49,4 1	1,01274 5	0,008	4,33	8,016 9	DOC
Samoylov; Polygon pond Mid	4.965	L17-11-8b	1,056 6	0,0081	-442, 4	1,06327	0,0084	54,4 3	8,354 2	DOC
Samoylov; Polygon pond South	7.626	L17-12-8b	1,062 6	0,0077	-488, 1	1,06918 9	0,0079	60,3	7,941 5	DOC
Kurung-nakh, Oval Lake Cen-ter; ~5m water depth	4.539	L17-13-8b 0m	0,700 0	0,0058	2865	0,69802 9	0,006	-308	5,996 6	DOC

Appendix 1: Prosecution of Appendix 1 (Table of used and measured samples; F^{14}C (measured values); F^{14}C cor (Blank corrected values); Δ^{14}C (Blank corrected).)

Location	Conc. [mg/L]	Sam-ple	F^{14}C	= + - (abs)	age (y)	F14C s cor	σF14C s	Δ14 C	σΔ14 C	Sam-ple
Kurungnakh, Oval Lake Center; ~5m water depth	4.505	L17-13-8b 2m	0,6995	0,0060	2871	0,697568	0,0062	-308	6,1683	DOC
Kurungnakh, Oval Lake Center; ~5m water depth	4.625	L17-13-8c 4m	0,6974	0,0061	2895	0,695339	0,0063	-310	6,3149	DOC
Kurungnakh, Oval Lake out-flow/Lucky Lake Inflow (downstream of Oval Lake)	4.547	L17-14-8c	0,7073	0,0062	2782	0,705417	0,0064	-300	6,3874	DOC
Kurungnakh, Lucky Lake Outflow	4.967	L17-15-8b	0,6526	0,0057	3428	0,649281	0,0059	-356	5,8693	DOC
Kurungnakh, outflow at coast (down-stream of Lucky Lake)	4.209	L17-16-8b	0,7072	0,0058	2783	0,704914	0,0061	-301	6,1208	DOC
Kurungnakh, Lucky Lake Center, ~4m water depth	5.009	L17-17-8b 0m	0,6397	0,0056	3589	0,636166	0,0058	-369	5,7523	DOC
Kurungnakh, Lucky Lake Center, ~4m water depth	4.986	L17-17-8b 1,5m	0,6378	0,0056	3613	0,634356	0,0058	-371	5,8017	DOC
Kurungnakh, Lucky Lake Center, ~4m water depth	5.039	L17-17-8c 3m	0,6349	0,0055	3649	0,631376	0,0057	-374	5,7429	DOC
Samoylov; North Lake, center;	1.378	L16-01a-3a	0,5720	0,0057	4487	0,728892	0,0372	-277	37,176	POC

Appendix 1: Prosecution of Appendix 1 (Table of used and measured samples; F^{14}C (measured values); F^{14}C cor (Blank corrected values); Δ^{14}C (Blank corrected).)

Location	Conc. [mg/L]	Sample	F^{14}C	= + - (abs)	age (y)	F14C s cor	σF14Cs	Δ14C	σΔ14C	Sample
Samoylov; North Lake, center; 3,7m	1.533	L16-01b-2a	0,5002	0,0053	5565	0,598426	0,0286	-407	28,645	POC
Samoylov; North Lake, outflow	6.933	L16-02-2c	0,9628	0,0074	304,9	1,014634	0,0101	6,2	10,147	POC
Samoylov; North lake, Polygon-1	1.556	L16-03-3a	0,6246	0,0059	3780	0,78012	0,0326	-226	32,574	POC
Samoylov; North Lake, Polygon-2	1.422	L16-04-2a	0,6504	0,0069	3456	0,842419	0,0395	-165	39,456	POC
Samoylov; North Lake, Polygon-3	2.200	L16-05-2b	0,7304	0,0064	2524	0,955294	0,0412	-52,6	41,241	POC
Kurungnakh;Lucky Lake, center;	0.611	L16-09a-2a	0,5735	0,0056	4467	0,692257	0,057	-314	57,045	POC
Kurungnakh;Lucky Lake, center; 2m	0.600	L16-09b-2a	0,6250	0,0060	3776	0,770658	0,0677	-236	67,743	POC
Kurungnakh;Lucky Lake, center; 3,5-3,7m	0.478	L16-09c-2a	0,6547	0,0062	3403	0,881402	0,1152	-126	115,2	POC
Kurungnakh;Lucky Lake, 50 to 70 m before outflow	0.678	L16-10a-2a	0,5859	0,0055	4294	0,693285	0,0495	-312	49,461	POC
Kurungnakh;Lucky Lake, 50 to 70 m before outflow	0.589	L16-10b-2a	0,5501	0,0056	4801	0,664412	0,0569	-341	56,933	POC
Kurungnakh;Lucky Lake, 50 to 70 m before outflow	0.522	L16-10c-2a	0,5553	0,0055	4726	0,695417	0,0725	-310	72,49	POC
Kurungnakh;Lucky Lake, outflow	0.411	L16-11-2a	0,5510	0,0055	4788	0,757587	0,1218	-249	121,83	POC

Appendix 1: Prosecution of Appendix 1 (Table of used and measured samples; F^{14}C (measured values); F^{14}C cor (Blank corrected values); Δ^{14}C (Blank corrected).)

Location	Conc. [mg/L]	Sample	F^{14}C	= + - (abs)	age (y)	F14C s cor	σF14C s	Δ14 C	σΔ14 C	Sample
Kurung-nakh;Lucky Lake, inflow	0.544	L16-12-2a	0,5812	0,0056	4360	0,726277	0,0721	-280	72,121	POC
Kurungnakh;Oval Lake, center	0.467	L16-13a-2a	0,5803	0,0061	4371	0,765547	0,0991	-241	99,057	POC
Kurungnakh;Oval Lake, center	0.533	L16-13b-2a	0,5566	0,0055	4707	0,692871	0,0698	-313	69,824	POC
Kurungnakh;Oval Lake, center	0.578	L16-13c-2a	0,5524	0,0057	4768	0,671072	0,0593	-335	59,346	POC
Samoylov; Flood Plain, outflow (North Lake study site)	1.267	L16-22-2a	0,7932	0,0066	1861	0,878254	0,0316	-129	31,59	POC
Samoylov, North Lake outflow	0.750	L17-01-4b	0,8791	0,0070	1035	0,939777	0,0137	-68	13,742	POC
Samoylov, North Lake center; ~4m water depth at sampling location	0.490	L17-04-7b 0m	0,8300	0,0072	1497	0,889281	0,0099	-118	9,8876	POC
Samoylov, North Lake center; ~4m water depth at sampling location	0.560	L17-04-7b 1.5m	0,8705	0,0072	1114	0,925312	0,0094	-82,4	9,4415	POC
Samoylov, North Lake center; ~4m water depth at sampling location	0.430	L17-04-7b 4m	0,8905	0,0074	931,7	0,966084	0,0112	-41,9	11,18	POC

Appendix 1: Prosecution of Appendix 1 (Table of used and measured samples; F^{14}C (measured values); F^{14}C cor (Blank corrected values); Δ^{14}C (Blank corrected).)

Location	Conc. [mg/L]	Sample	F^{14}C	= + - (abs)	age (y)	F14C s cor	σF14C s	Δ14 C	σΔ14 C	Sam -ple
Samoylov Katya Lake (on flood-lplain downstram of North Lake)	0.920	L17-05-7b	0,7941	0,0067	1852	0,822398	0,0075	-184	7,5349	POC
Samoylov; Outflow floodplain to Lena, down-stream of Katya Lake	0.380	L17-06-7b	0,8872	0,0072	961,6	0,973624	0,012	-34,5	12,006	POC
Samoylov; Polygon pond North	1.080	L17-10-7b	0,8734	0,0073	1087	0,930691	0,0097	-77	9,7174	POC
Samoylov; Polygon pond Mid	1.040	L17-11-7b	0,8897	0,0073	938,7	0,950917	0,01	-57	9,9884	POC
Samoylov; Polygon pond South	0.900	L17-12-7b	0,8734	0,0073	1087	0,943408	0,0107	-64,4	10,718	POC
Kurung-nakh, Oval Lake Center; ~5m water depth	0.620	L17-13-7b 0m	0,7615	0,0064	2189	0,802028	0,008	-205	7,9583	POC
Kurung-nakh, Oval Lake Center; ~5m water depth	0.650	L17-13-7b 2m	0,7575	0,0065	2231	0,795739	0,0079	-211	7,9003	POC
Kurung-nakh, Oval Lake Center; ~5m water depth	0.510	L17-13-7c 4m	0,7649	0,0069	2153	0,815309	0,0091	-191	9,0667	POC

Appendix 1: Prosecution of Appendix 1 (Table of used and measured samples; F^{14}C (measured values); F^{14}C cor (Blank corrected values); Δ^{14}C (Blank corrected).)

Location	Conc. [mg/L]	Sam-ple	F^{14}C	= + - (abs)	age (y)	F14C s cor	σF14C s	Δ14 C	σΔ14 C	Sam-ple
Kurungnakh, Oval Lake out-flow/Lucky Lake Inflow (downstream of Oval Lake)	0.580	L17-14-7c	0,7780	0,0066	2017	0,822895	0,0084	-184	8,3829	POC
Kurungnakh, Lucky Lake Outflow	0.280	L17-15-7b	0,6867	0,0074	3019	0,771547	0,0128	-235	12,834	POC
Kurungnakh, outflow at coast (down-stream of Lucky Lake)	7.3	L17-16-7b	0,5727	0,0053	4478	0,57678	0,0054	-428	5,4129	POC
Kurungnakh, outflow at coast (down-stream of Lucky Lake)	13.44	L17-16-7b	0,5935	0,0054	4191	0,595854	0,0055	-409	5,4858	POC
Kurungnakh, Lucky Lake Center, ~4m water depth	0.940	L17-17-7c 0m	0,6007	0,0057	4094	0,618625	0,0063	-387	6,2904	POC
Kurungnakh, Lucky Lake Center, ~4m water depth	0.750	L17-17-7b 1.5m	0,7262	0,0066	2570	0,75697	0,0076	-249	7,6003	POC
Kurungnakh, Lucky Lake Center, ~4m water depth	0.590	L17-17-7c 3m	0,6983	0,0061	2884	0,735881	0,0076	-270	7,6398	POC
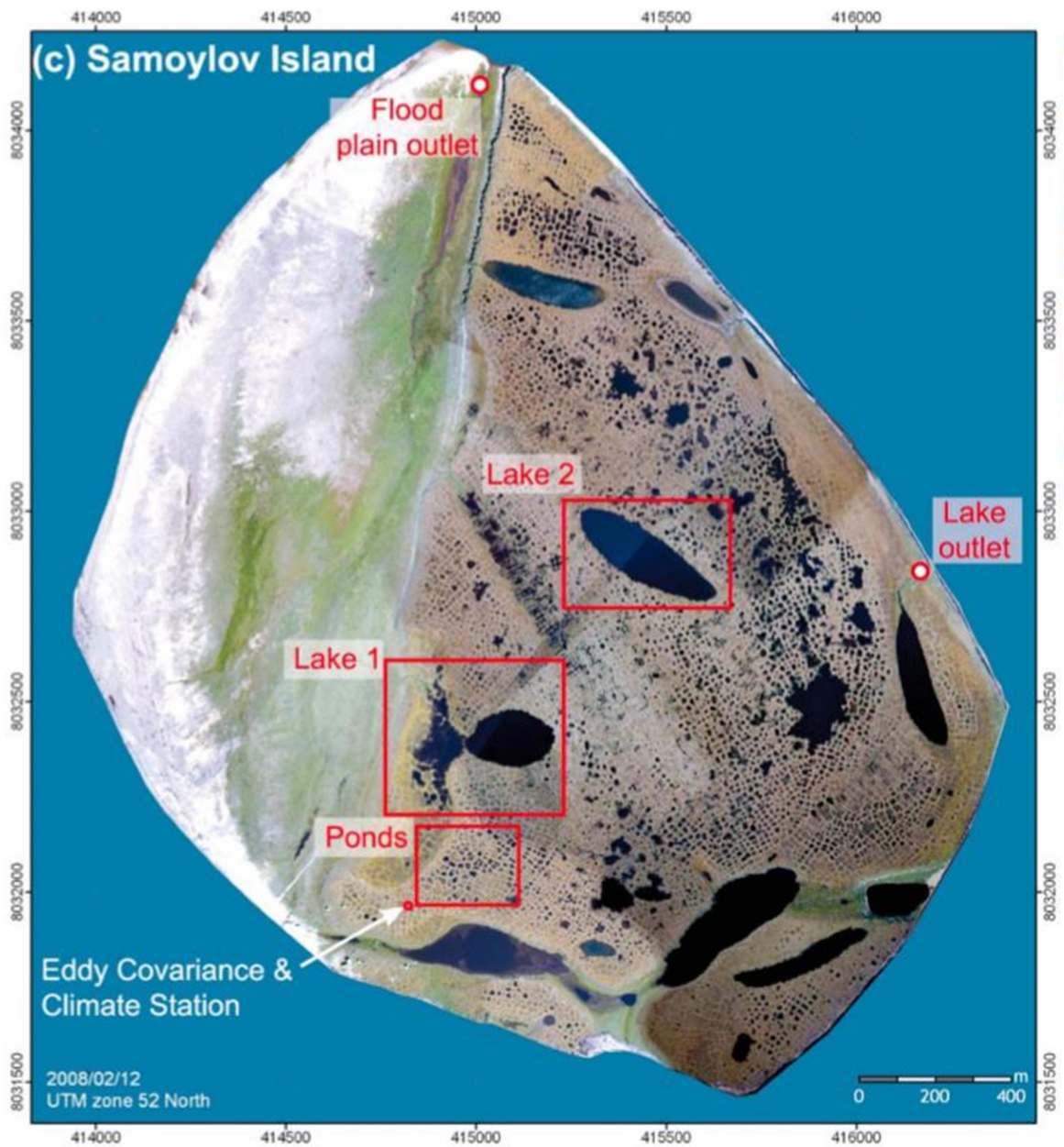
Appendix 2: Satellite image of Abnizovas sampling locations (Abnizova et al. 2012)

	Thermokarst Lake 1	Thermokarst Lake 2	Pond 1	Pond 2	Lake Outlet	Floodplain Outlet
Trophic state	Oligotrophic	Oligotrophic	Oligotrophic	Oligotrophic		
Latitude N	8032363	8032778	8031992	8031981	8032840	8034141
Longitude E	414855	415607	414946	414928	416191	415027
Volume (m³)	104820	96829	70	12	-	-
Surface area (m²)	45982	40714	221	130	-	-
Area/Volume	0.44	0.42	3.16	10.54	-	-
Maximum depth (m)	6.40	5.7	0.18	0.5	-	-
Ca (mg/l)	7.5	6.7	4.6	14.5	6.2	29.0
	8.8(2.4–9.2)	6.9(5.8–7.0)	5.1(2.4–6.2)	15.4(7.2–25.8)	6.1(3.1–7.9)	n/a(23.8–34.5)
Mg (mg/l)	3.4	3.3	3.2	7.9	3.0	12.3
	4.0(1.0–4.1)	3.5(2.9–3.5)	3.6(1.6–4.1)	8.7(4.6–12.2)	3.0(1.5–3.8)	n/a(11.0–13.9)
Na (mg/l)	2.6	0.6	0.6	1.1	1.5	1.6
	3.1(0.8–3.1)	0.7(0.5–0.7)	0.7(0.3–0.8)	1.2(0.8–1.3)	1.5(0.7–1.8)	n/a(1.2–2.1)
K (mg/l)	0.6	0.5	0.9	0.7	0.4	0.4
	0.6(0.4–0.9)	0.6(0.4–0.6)	1.2(0.4–1.1)	0.8(0.3–0.9)	0.5(<0.2–0.4)	n/a(0.3–0.5)
Fe (µg/l)	105.0	21.3	211.4	907.9	301.0	359.3
	94.9(42.8–180.0)	23.2(<20–49.5)	134.0 (114.0–506.0)	231.0(114.0–2660.0)	118.0(118.0–727.0)	n/a (234.0–570.0)
Mn (µg/l)	<20	<20	<20	413.1	49.7	343.5
	<20(<20–<20)	<20(<20–<20)	<20(<20–<20)	53.1(<20–1500)	<20(<20–139.0)	n/a (32.4–782.0)
Si (mg/l)	0.3	0.3	0.4	2.1	0.6	2.0
	0.5(<0.1–0.5)	0.3(0.2–0.5)	0.7(<0.1–0.7)	4.7(0.5–3.0)	0.7(0.2–1.0)	n/a (1.5–2.2)
Sr (µg/l)	43.1	33.5	29.6	78.0	31.8	155.8
	50.0(<20–53.1)	33.4(29.4–35.4)	31.0(<20–42.2)	84.5(52.5–98.9)	31.8(<20–41.3)	n/a (109.0–198.0)
Cl (mg/l)	3.7	0.7	0.7	0.9	1.8	0.4
	3.8(2.9–4.4)	0.7(0.6–0.7)	0.9(0.6–0.9)	1.5(0.4–1.1)	1.9(1.3–2.0)	n/a (<0.1–0.8)
SO$_4$ (mg/l)	1.8	0.1	<0.1	<0.1	0.7	0.1
	1.9(1.2–2.0)	<0.1(<0.1–0.1)	<0.1(<0.1–<0.1)	<0.1(<0.1–<0.1)	0.8(0.5–0.9)	n/a 0.1–0.5)
Alkalinity (mmol/l)	0.8	2.3	0.9	1.5	0.7	n/a
Conductivity (µS/cm)	92.2	65.5	57.7	121.6	69.0	255.4
	92.0 (86.0–100.0)	66.0 (63.0–67.0)	60.0 (53.0–61.0)	126.0 (78.0–225.0)	65.0 (64.0–80.0)	n/a (208.0–307.0)
DO (mg/l)	7.8	10.0	7.2	5.2	9.5	6.1
	8.8(6.8–8.9)	9.1(8.3–14.6)	7.6(4.5–9.9)	5.5(2.1–8.3)	9.4(7.0–13.9)	n/a (3.1–9.7)
DOC (mg/l)	4.0	2.1	4.2	6.8	2.8	4.3
	4.0(2.8–5.6)	2.6(1.7–2.6)	4.2(3.1–5.4)	7.4(4.2–14.4)	3.3(1.9–3.8)	n/a (2.6–6.5)
DIC* (mg/l)	13.1	8.3	13.6	25.0	11.6	41.8
	13.2(11.6–14.4)	7.8(7.0–10.2)	22.3(9.2–22.3)	45.4(12.5–45.4)	14.8(9.3–14.8)	n/a (40.3–43.2)
pH	7.2	7.2	6.8	7.2	7.3	7.5
	7.2(6.9–7.3)	7.4(7.2–7.4)	6.5(6.5–7.1)	6.8(6.8–7.5)	7.8(7.0–7.8)	n/a (7.5–7.5)
N$_2$O-N* (µg/l)	0.46	0.42	0.26	0.31	0.44	0.43
	0.53(0.39–0.53)	0.38(0.38–0.45)	0.00(0.00–0.42)	0.0(0.00–0.47)	0.41(0.41–0.49)	n/a (0.39–0.47)
δ^{18}O (‰)	-17.4	-16.8	-14.7	-15.9	-17.8	-16.8
	-16.3(-17.8—16.3)	-16.8(-17.0—16.7)	-15.4(-15.4–14.3)	-17.7(-17.7—13.9)	-18.0(-18.3—15.7)	n/a -18.4—15.7)
δD (‰)	-136.4	-133.5	-122.2	-125.9	-140.1	-131.0
	-129.1(-139.0—129.1)	-132.6(-134.7—132.2)	-124.9(-124.9—120.7)	-136.2(-136.2—119.3)	-140.9(-143.7—124.7)	n/a (-137.9—125.0)

Olga Ognevas Samples from the Lena River				
coordinates	N 72°23´59.3''	E 126°42´22.0''		
Date of sampling 2017	11.07.2017			
Date of sampling 2016	15.08.2016			
Sample ID	Filtration	depth [m]	**DOC, mg/L**	Δ14C
L17-08-0m	0.75	0	4,995	55
L17-08-12m	0.75	12	6,459	63
L17-08-21m	0.75	21	6,408	56
L16-15-02m	0.75	2	8,264	59
L16-15-12m	0.75	12	8,045	36
L16-15-20m	0.75	21	8,202	60

Appendix 5: Sample locations of this thesis and Olga Ognevas Lena sample (red arrow)